'MENTATION PAGE

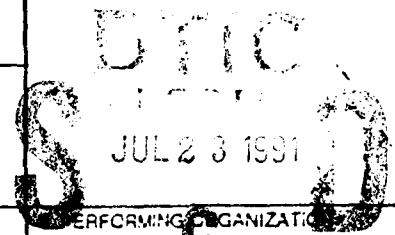| 2. REPORT DATE	3. REPORT TYPE AND DATES COVERED
1 June 1991	Masters Thesis 5 Sept 89 - 1 Jun 91

4. TITLE AND SUBTITLE

Ocean Thermal Feature Recognition, Discrimination and Tracking using Infrared Satellite Imagery

5. FUNDING NUMBERS

6. AUTHOR(S)

James A. Holland II, Major, U.S. Army

7. PERFORMING ORGANIZATION NAME(S) AND ADDRESS(ES)

USASD, Ft. Benjamin Harrison, IN 46216-5820, W/DY
Dept. of Electrical Engineering, University of
Delaware, Newark, DE 19716

8. PERFORMING ORGANIZATION REPORT NUMBER

9. SPONSORING/MONITORING AGENCY NAME(S) AND ADDRESS(ES)

10. SPONSORING MONITORING AGENCY REPORT NUMBER

11. SUPPLEMENTARY NOTES

This document was prepared in order to satisfy the requirements for the conferral of a Masters Electrical Engineering Degree from the University of Delaware.

12a. DISTRIBUTION/AVAILABILITY STATEMENT

Distribution Unlimited

12b. DISTRIBUTION CODE

13. ABSTRACT (Maximum 200 words)

This paper presents a method to quantitatively measure ocean surface movement, using 10.5 micron band AVHRR images. An ordered statistical edge detection algorithm is used to select thermal pattern features, at the same time discriminating between the water surface, clouds and land. A constrained statistical correlation based recognition scheme is then used to find the best match to the pattern feature in a subsequent image. Study Areas off the Delaware and New Jersey coast were analysed using this method, with results comparing favorably with in situ anchored buoy measurements. All relevent algorithms are included in the paper with key program code included in appendices.

14. SUBJECT TERMS

Remote Sensing, Satellite Imagery, Thermal Imagery, Pattern Recognition, Motion Estimation, Current Estimation

15. NUMBER OF PAGES

16. PRICE CODE

17. SECURITY CLASSIFICATION OF REPORT	18. SECURITY CLASSIFICATION OF THIS PAGE	19. SECURITY CLASSIFICATION OF ABSTRACT	20. LIMITATION OF ABSTRACT
UNCLASSIFIED	UNCLASSIFIED	UNCLASSIFIED	Unlimited

OCEAN THERMAL FEATURE

RECOGNITION, DISCRIMINATION

AND TRACKING

USING

INFRARED SATELLITE IMAGERY

by

James A. Holland II

A thesis submitted to the Faculty of the University of Delaware in partial fulfillment
of the requirements for the degree of Master of Electrical Engineering

June 1991
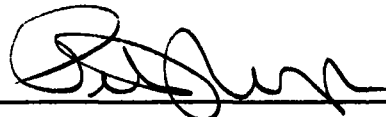
91 7 19 067
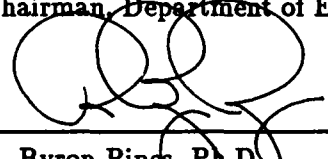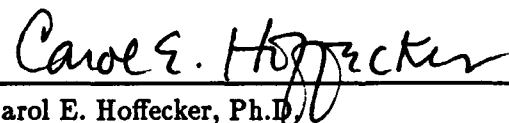
OCEAN THERMAL FEATURE

RECOGNITION, DISCRIMINATION

AND TRACKING

USING

INFRARED SATELLITE IMAGERY

by

James A. Holland II

Approved: _____

Charles G. Boncelet, Ph.D.
Professor in charge of thesis on behalf of the Advisory Committee

Approved: _____

Peter J. Warter, Ph.D.
Chairman, Department of Electrical Engineering

Approved: _____

R. Byron Pipes, Ph.D.
Dean, College of Engineering

Approved: _____

Carol E. Hoffecker, Ph.D.
Acting Associate Provost for Graduate Studies

ACKNOWLEDGMENTS

PREFACE

For my wife, Heather, and my daughter, Karlynn, who have spent many long hours waiting for this soldier and student.

TABLE OF CONTENTS

Chapter

LIST OF FIGURES

ix

x

LIST OF TABLES

ABSTRACT

Sea surface motion has been observed for two decades by viewing successive satellite thermal infrared images for movement of thermal gradients. A major effort has been made over the last eight years to automate the task of measuring surface current flow using satellite images, a task made difficult by the presence of land, clouds and other unwanted features.

This paper presents a method to quantitatively measure ocean surface movement. Using 10.5 μm band imagery, sequential images are processed, correcting for the presence of clouds and land, to determine flow direction, magnitude, and velocity. An ordered statistical edge detection algorithm is used to detect gradient boundaries, discriminate between the water surface, land and clouds, and select thermal features. A constrained correlation based pattern recognition scheme is then used to match the feature in the next image. Surface flow is calculated for each selected point with results presented in tabular and image form. A study area in the region of the Delaware Bay, on the east coast of the United States, has been analyzed using this technique, with the results comparing favorably with *in situ* anchored buoy measurements.

Chapter 1

INTRODUCTION

1.1 Purpose

Imaging satellites provide viewing of the earth's surface in temporal and spatial scales that cannot be matched by surface bound collection methods. Modeling of the world's oceans mixed layer depths, a vital ocean region for primary production of food and oxygen, is very dependent on surface current information. At present, most of this information is available only from ships, research vessels and anchored or free floating buoys. These platforms have small observation areas, providing only the most limited coverage of the ocean surface.

This work was initiated to provide the Center for Remote Sensing, University of Delaware, with a method to objectively process satellite thermal images to estimate sea surface velocity.

1.2 Use of satellites to view the earth surface

Images collected and sent by satellites offer unprecedented viewing of the planet we live on. Satellites in orbit today for civil applications are viewing the earth with visible, near infrared, thermal infrared and radar sensors. Figure 1.1 illustrates the key concepts of satellite imaging of the earth's surface.

Geostationary (GOES) satellites are placed in a very high orbit above the earth (approximately 36,000 km) to have their orbit match the earth's rotation rate. This allows viewing of the same area at all times, but limits resolution to very large features.

Low orbiting satellites (500-2,000 km) travel around the earth at velocities relating to their altitude. Most mapping satellites, including the ones that provided the images

1
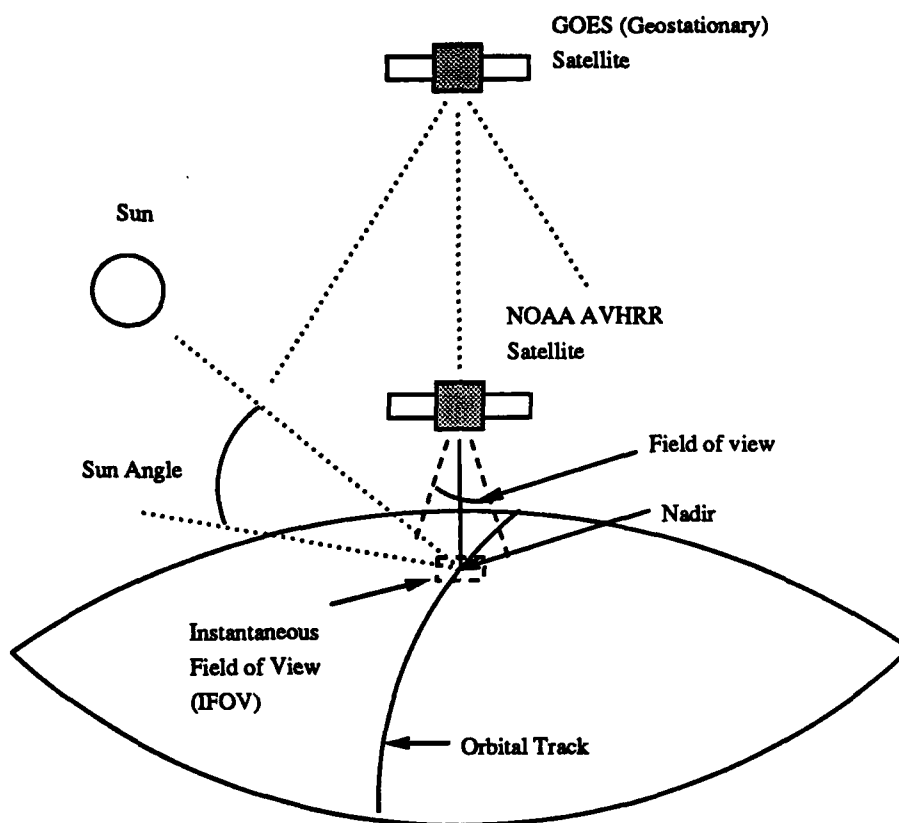
Figure 1.1: Low orbiting and geostationary satellite comparison.

for this study, are in low polar orbits where the earths rotation moves perpendicular to the satellite path, allowing coverage of a portion or the entire surface over time.

1.3 Satellite imagery used in this study

This paper uses images from National Oceanic and Atmospheric Administration (NOAA) low orbiting satellites, NOAA - 8, 9 and 10. The images used in this study are from the 10.5 μm band, Advanced Very High Resolution Radiometer (AVHRR) sensor. They are in a 512×512 pixel format, and are geometric and grey scale value for temperature corrected, with a nominal pixel dimension of 1.1 kilometers at the nadir. From a series of images covering the period 1 January to 30 June 1989, sets acceptably free from clouds were selected for the following periods:

- 10-11 March 1989.

- 28-29 May 1989.

- 10-12 June 1989.

- 29-30 June 1989.

The images are stored in 8 bit, 0-255 value, grey scale form. Ocean thermal features are visible as gradients (Figure 1.3). Temperature can be determined from the image using a linear function with a slope of 0.125 and a y intercept of zero in the form:

$$T = V_{pixel} \times 0.125 \, . \tag{1.1}$$

This gives the image a scaling temperature range from 0 - 32° Centigrade (C). Features with surface temperatures above or below this range are treated as sensor saturating signals and are assigned 255 or 0 respectively (Figure 1.2).

1.4 Principles of ocean surface flow estimation

The work of Vastano and Reid [1], categorizing surface flow in the Oyashio Frontal Zone in the northwest Pacific Ocean was the starting point for this project. Their observations using AVHRR (11μm band) images showed an 11° centigrade (C) temperature variation in Sea Surface Temperature (SST). They observed defined regions of temperature which they associated with frontal regions of differing streamflow. These temperature gradients are produced by "small scale waves or turbulent processes ... of (what should be) otherwise smooth surface isotherms."

Rossby like internal gravity waves, the effects of heat exchange with the atmosphere, and vertical motion on the sea surface were assumed to produce much smaller changes in SST than the turbulance caused by currents which bring core temperatures to the surface.

1.4.1 Surface flow model

Rossby like waves have a length and time scale described by [2]:

$$L = \frac{DN_0}{f_0} \, ,$$
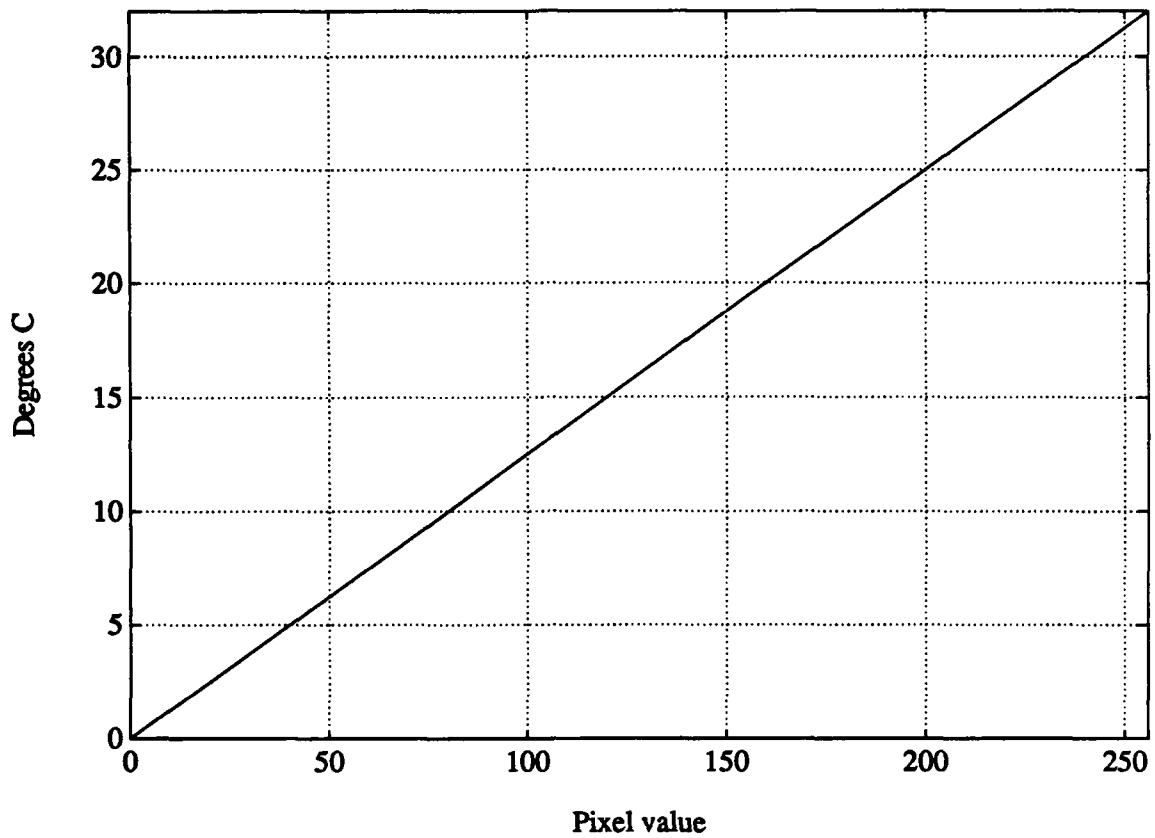
Figure 1.2: NOAA thermal image temperature scale. One pixel value equals a change of 0.125 degrees centigrade.

and

$$T = \frac{2\pi \ R \ tan\theta}{N_0 \ D} \ ,$$

where L is the Rossby scale of horizontal motion, N_0 is the characteristic buoyancy, D is the vertical scale characteristic, f_0 is the coriolis parameter, R is the radius of the earth, and θ is the latitude.

Using values from Stewart [2], for 40° North (the region of interest for the images analyzed in Vastano's study) yields:

$$L = 74 \ km,$$
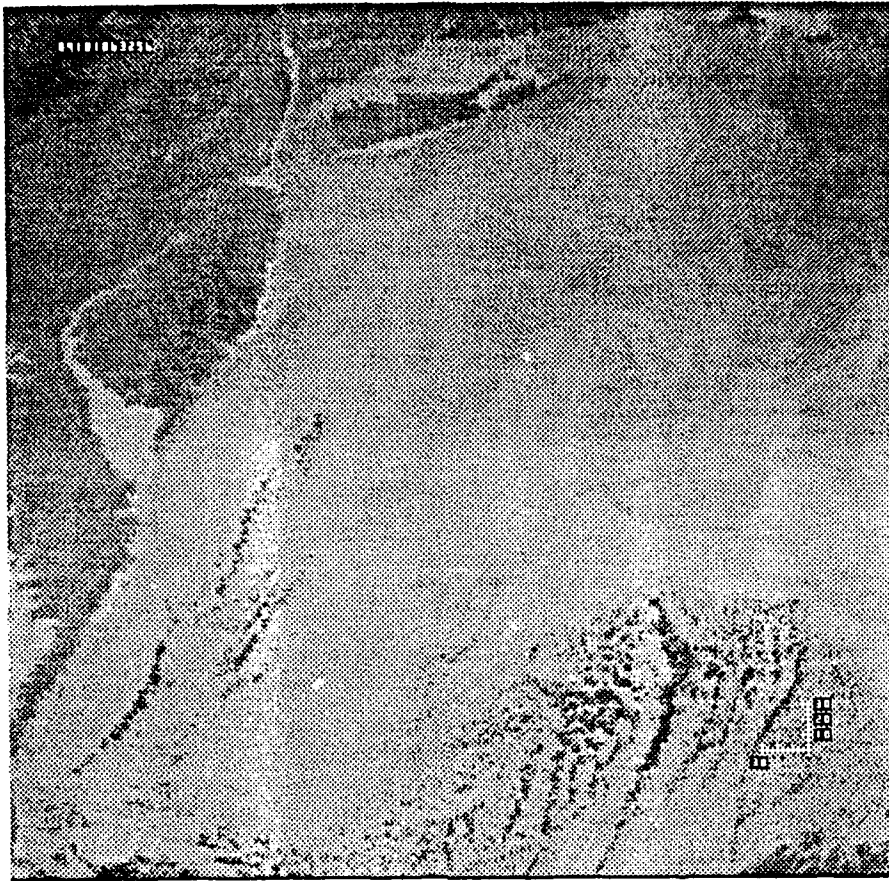
Figure 1.3: Typical satellite thermal image of coastal Delaware and the continental shelf. 0132 hours local, 30 June 1989 (false color added for feature enhancement).

$$T = 83 \; days,$$

$$Flow_{Rossby} = 0.011 \; m/s.$$

For study of the Delaware - New Jersey coastal area (30° North), with measured flows of 0.1 to 1.2 meters per second, Vastano's assumption to ignore Rossby waves still applies, since $Flow_{Rossby} \approx 0.013$ m/s.

In Vastano and Reid's paper, local changes in sea surface temperature are described with the following model:

$$\frac{dC}{dt} = \frac{\partial C}{\partial t} + V \cdot \nabla C = R, \tag{1.2}$$

where C represents atmosphere heat exchange, diffusion and vertical motion perturbation components, V is the perturbation due to flow and R is the rate of temperature change.

C and V each have two components:

$$C = C_0 + C_1 \,, \tag{1.3}$$

$$V = V_0 + V_1 \,, \tag{1.4}$$

where C_0 and V_0 are mean components of change and C_1 and V_1 represent the perturbation effects.

Expanding equation 1.2 with 1.3 and 1.4 yields:

$$\partial C_1 = R - V_0 \cdot \nabla C_1 = S_1 + S_2 \,, \tag{1.5}$$

where S_1 is the self advective, turbulent diffusion term. Expanding S_1 to represent effects of wind, convection and internal waves:

$$S_1 = R - V_0 \cdot \nabla C_0 - V_1 \cdot \nabla C_1 - \frac{dC_0}{dt} \,. \tag{1.6}$$

S_2 is the temperature change due to flow:

$$S_2 = -V_1 \cdot \nabla C_0 \,, \tag{1.7}$$

Using the observation that the mean terms of C and V change slowly, relative to the rapid changes of temperature over distance and time on the flow boundaries, equation 1.6 is disregarded. This leaves equation 1.7 as the representing source term to describe changes in Sea Surface Temperature.

Away from flow boundaries this change can be described by:

$$\frac{\partial C_1}{\partial t} + V_0 \cdot \nabla C_1 = 0 \,, \tag{1.8}$$

where the velocity V_0 represents the velocity of small discrete volumes of water. This velocity is assumed to be equivalent to the time rate of change of the displacement of the parcel between sampling periods (images).

Assuming the flow is horizontally nondivergent and using an approximation of a uniform Coriolis parameter, Vastano concluded that the surface velocity can be approximated by a single scalar streamfunction, Ψ. This function is represented in trigonometric terms by:

$$\Psi = \sum_n \sum_m A_{n,m} \sin \frac{n\pi x}{L_x} \sin \frac{m\pi y}{L_y}, \tag{1.9}$$

where L_x and L_y are the dimensions of the region surrounding the samples.

The vertical (u) and horizontal (v) velocity components are derived from:

$$u = -\frac{\partial \Phi}{\partial y} = -\sum_n \sum_m \frac{m\pi}{L_y} A_{n,m} \sin \frac{n\pi x}{L_x} \cos \frac{m\pi}{L_y}, \tag{1.10}$$

$$v = +\frac{\partial \Phi}{\partial x} = -\sum_n \sum_m \frac{n\pi}{L_x} A_{n,m} \cos \frac{n\pi x}{L_x} \cos \frac{m\pi}{L_y}. \tag{1.11}$$

1.4.2 Additional considerations for the Vastano and Reid model

Wahl and Simpson [3], have shown that the assumptions of the Vastano and Reid model concerning horizontal diffusion and changes in Sea State Temperature (SST) are in error. At wind surface wind speeds less than 10 *meters/second* (*m/s*), horizontal *as well as* vertical diffusion, and air - sea heat exchange are the dominant process in SST change. Surface winds greater than 20 *m/s* usually cause intense vertical mixing, destroying the thermal feature. Work by Price [4] has shown that diurnal heating also causes significant distortion of thermal features by wind stress induced *diurnal jets* which transport surface thermal features normal to wind direction at velocities up to 0.1 *m/s* for moderate winds.

The conservation of heat equation now becomes:

$$\frac{dT}{dt} = K_h \nabla_H^2 T + K_z \frac{\partial^2 T}{\partial z^2} + \sum_i Q_i , \qquad (1.12)$$

where $\frac{dT}{dt}$ is the material derivative of temperature over time, K_H is the horizontal diffusivity, Q_i is the heating source (or sink) term, T is the temperature, an t is time. The derivative of temperature is defined by:

$$\frac{dT}{dt} = \frac{\partial T}{\partial t} + u \cdot \nabla T , \qquad (1.13)$$

where $u = (u, v, w)$ is the fluid velocity. For a two - dimensional, non - compressible flow, assuming a *well mixed layer* ($\frac{\partial T}{\partial z} \ll \frac{\partial T}{\partial x}$) and ($\frac{\partial T}{\partial z} \ll \frac{\partial T}{\partial y}$), $\frac{dT}{dt}$ becomes:

$$\frac{dT}{dt} = U \cdot \nabla T + K_H \nabla_H^2 T + \sum_i Q_i , \qquad (1.14)$$

where the first term, $U \cdot \nabla T$, is the advection term, the second term, $K_H \nabla_H^2 T$, is the horizontal diffusion term and the last term, $\sum_i Q_i$ represents the air - sea interaction.

1.5   The validity of surface feature duration assumptions

The fundamental assumption which allows estimation of surface flow from satellite imagery is that the thermal feature, representing the temperature of a volume of water, remains relatively intact during the sampling interval. Each pixel represents 1.21 square kilometers (km^2) or greater of sea surface. The latent heat flux calculated using satellite data represents the majority of the temperature of a layer of homogeneous temperature water, called the *surface mixed layer*. This mixed layer may extend to depths of a few hundred meters in winter, to less than 40 meters in summer.

The critical assumption which allows satellite determination of surface flow is that thermal features sampled over a large area (a 10 × 10 pixel sample is an area greater than 127 km^2), retain their three dimensional identity over periods of up to 24 hours. This assumption corresponds to one consecutive pass by a single low orbit satellite over the same location. This is true as long as surface flow is dominated by by geostropic currents, resulting in only advective motion in the horizontal plane, with little or no horizontal

diffusion. The presence of wind driven diurnal currents, giving K_H velocities of 5 - 10 cm/s casts some question as to the validity of the assumption that horizontal diffusion is minor term. Answering this question is beyond the scope of this work. The assumption $K_H\nabla^2_H T \ll U \cdot \nabla T$ is considered valid for periods less than 24 hours.

Chapter 2

THERMAL FEATURE SELECTION AND TRACKING

2.1 Feature selection

Using the assumption that a large volume of water will hold a distinctive thermal signal shape over time, it is possible to employ pattern recognition techniques to measure displacement of features defined by temperature alone. Once features are selected from an initial, or pattern image, motion can be estimated by locating them and measuring their displacement in subsequent images. In this work, this accomplished in three steps: Pattern features are first selected from an initial image using Ordered Statistical Edge Detection or, for comparison to other models, grid sampling methods. Use of edge detection to extract features insures that only areas of gradient change are mapped, eliminating samples of featureless areas that grid methods produce. Second, feature recognition, classification and selection are performed using a comparison image, searching areas having maximum likelihood of containing the matching pattern. As the last step, displacement, direction and velocity calculations are made based on movement of the matched features relative to the pattern features using a common coordinate system.

Edge detection (Figure 2.1) was employed to select features that are involved in advective flow across the sea surface, as opposed to more standard grid methods used by Kelly [5] and Simpson [6], to locate areas of maximum flow. This approach reduces the number of points selected, with a corresponding reduction in the number of calculations required to process an image. Figure 2.2 shows a three - dimensional representation of the thermal signal for the Delaware Bay mouth and coastal area, one of the areas of interest to this study. Feature selection maps an area of this signal, discriminating against selection of land, clouds and other unwanted features.

10
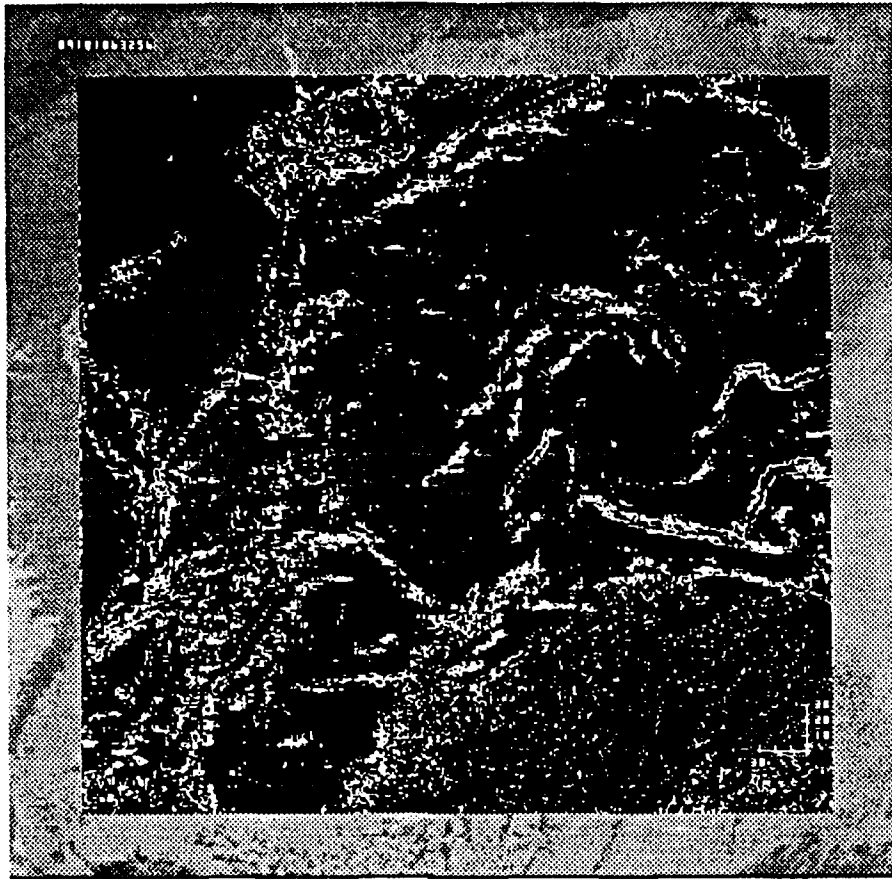
Figure 2.1: Thermal features detected by the SEDA method, superimposed on Figure 1.3, using a 5×5 edge detection tile (*Threshold* = 6, *Range* = 12).

2.1.1 Ordered statistical edge detection

The Ordered Statistical Edge Detection Algorithm (SEDA) which is used for feature selection is one adapted from the work of Hardie and Gnacek [7], based on the paper by Pitas and Venetsanopoulos [8]. This type of edge detector has proven to be very effective in noisy signal environments. The SEDA method is not orientation dependent. Even though it scans from left to right, it accurately detects ascending and descending gradients. marking curved and linear features. The method is very effective in locating features in noisy signal environments. It works by incrementally moving an $n \times n$ tile across an image looking for thermal gradients shown by contouring in Figure 2.3.

Using the SEDA method, each pixel is defined by a vector in a set of n vectors

Cape May, New Jersey
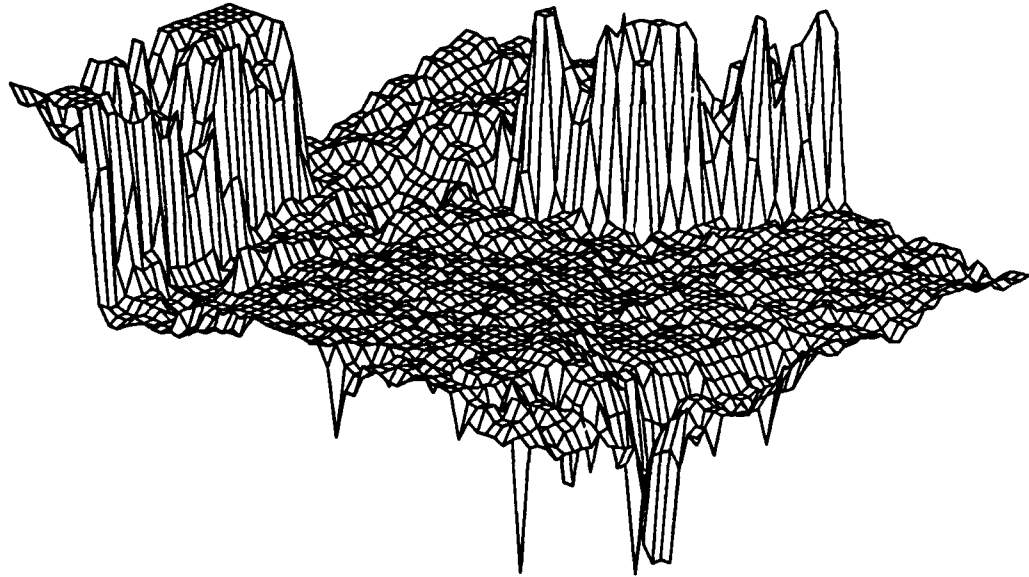
Thermal map: arbitrary scale, Azimuth: 315

Figure 2.2: Three dimensional thermal signal map, 1258 hours local, 30 June 1989, Delaware Bay and coast. The high values correspond to land temperatures for Cape May, New Jersey, and the coast near Lewes, Delaware. The very low values in the lower right corner are light cumulus clouds. The water temperature signal varies considerably from the Delaware Bay (upper left, behind Cape May), to the ocean waters in the foreground. The effects of turbulent mixing can be easily seen in the bay and its mouth as noticeable perturbations in surface signal.

Cape May, New Jersey
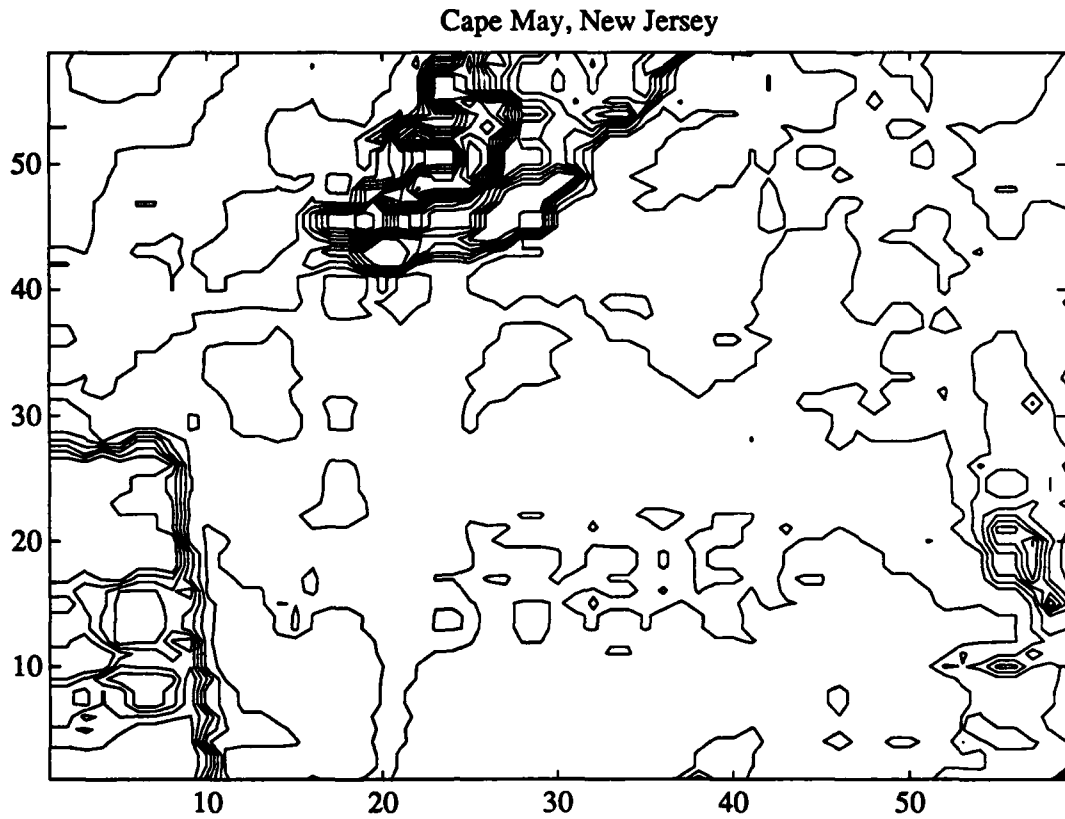
Thermal Contour: arbitrary scale

Figure 2.3: Thermal signal contour map, Delaware Bay and coastal region, 1258 hours local 30 June 1989. Cape May is the center top. Coastal Delaware is on the lower left. Light clouds can be observed on the lower right.

defined by the image dimensions such that:

$$W_n = a_1, a_2, ..., a_n .$$

Each vector sample is a set of n vectors defined by the edge detection tile dimensions:

$$a = [a_1, a_2, ..., a_n]^T .$$

The distance or value of the vector is the pixel value (0 - 255):

$$d_n = \|a_n\| .$$

As the edge detection tile moves across its search area, it generates a set of vectors:

$$a_1, a_2, ..., a_n ,$$

with values:

$$d_1, d_2, ..., d_n .$$

After rank ordering from highest to lowest, the set notation changes to:

$$a_{(1)} \leq a_{(2)} \leq \cdots \leq a_{(n)} ,$$

with vector $a_{(n)}$ having the largest value of d.

The SEDA algorithm selects an edge, δ, when the range exceeds a specified value, called a *Threshold* (T), represented in equation form by:

$$\delta(\cdot) = \begin{cases} 1 & \text{if range} > \text{T} \\ 0 & \text{otherwise} \end{cases} , \qquad (2.1)$$

with the range defined as:

$$range = a_{(n-i)} - a_{(1+i)} .$$

The value i is the number of ordered statistics chosen toward the mean to evaluate the sample and n is the number of pixels. The *range* value is the minimum change in intensity (pixel value) required to define the feature as an edge. Allowing $i = 1$, for example, selects edges based on $n - 2$ samples, ignoring the two opposite extreme values. The feature will be recorded if the $a_{(n-i)} - a_{(1+i)}$ value is greater than the specified T. The value of i used determines the type of edge selected. As i approaches $n/2$, the edge selected increases in relative sharpness, defined as an increasingly steep slope in the linear expression of the feature pixel values. Since the *range* criteria must be met with a difference calculated from a decreasing set of points, the slope must increase. A small value of i compared to n will select smoother, less sharp edges. A value of $i = 1$ was used in this study.

2.1.2   SEDA feature discrimination

The SEDA algorithm was modified during this project to allow it to discriminate between ocean thermal gradient patterns and undesirable features such as cloud and land masses. These methods are not one hundred percent effective, but do significantly reduce feature selection error. Figure 2.4 shows pattern tiles mapped for a study of the Delaware coastal region selected using the edge detection method. The method selected water features, except for tile 00 which was chosen in an area of light clouds.
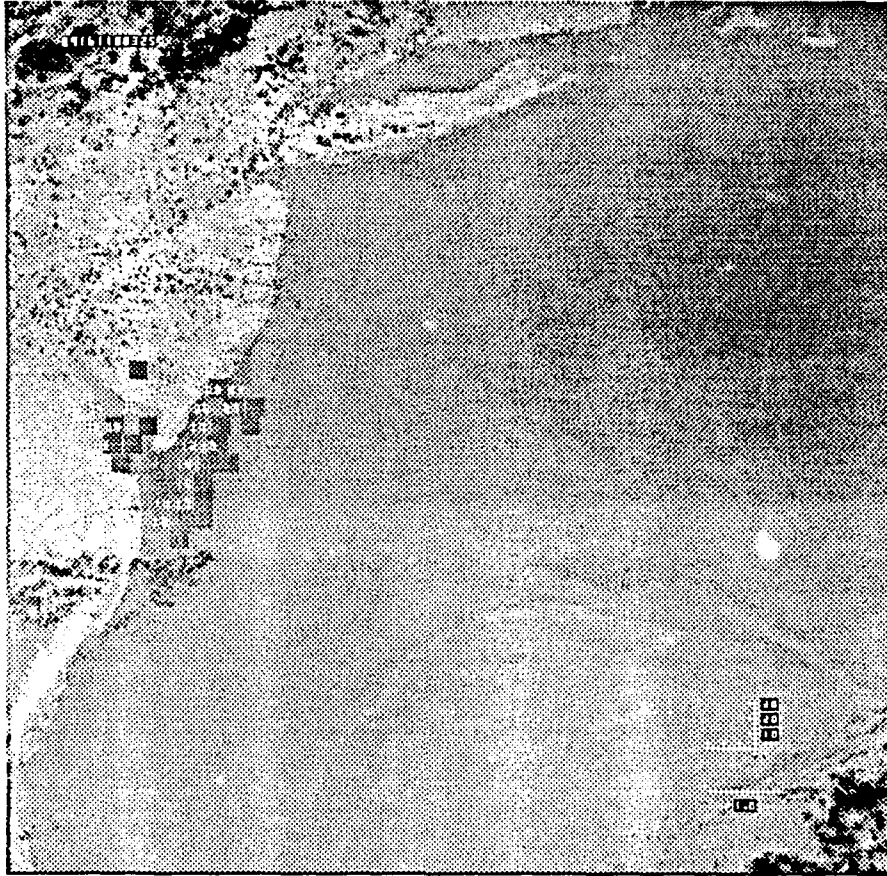
Figure 2.4:   Pattern tile selection in the Delaware Bay and coastal region, 1303 hours local. 10 June 1989, using the SEDA method. One false detection, tile 00, north of the bay was caused by light clouds. The scale in the lower right is the distance in kilometers. The arrow represents displacement for a flow rate of one meter per second.

The modification places additional restrictions to equation 2.1 to take advantage

Table 2.1: Typical values for feature selection classification.

Operator	Value	Use
range	6	Minimum Threshold: change must be greater than 0.75° C.
range$_{max}$	12	Maximum Threshold: change must not be greater than 1.5° C.
mask$_1$	131	Minimum Pixel Value: lowest ranked pixel must be greater than this value (summer ≈ 16.4° C).
mask$_2$	177	Maximum Pixel Value: highest ranked pixel must be less than this value (summer ≈ 22.13° C).

of the large differences in pixel values between the ocean and other features. The new selection algorithm is described by:

$$\delta(\cdot) = \begin{cases} 1 & \text{if } T < \text{range} < range_{max} \\ & \&\ a_{(1+i)} > mask_1 \\ & \&\ a_{(n-i)} < mask_2 \\ 0 & \text{otherwise} \end{cases} , \qquad (2.2)$$

where $range_{max}$ specifies a maximum change that can occur across a sample, $mask_1$ is the minimum allowed pixel value, and $mask_2$ is the maximum allowed pixel value.

$Mask_1$ and $mask_2$ are determined from sampling water temperatures in the area of interest and applying an allowed deviation factor. $Range_{max}$ and *range* provide a constraint to the maximum allowed change in apparent temperature. Table 2.1 shows some typical values.

2.1.3 Feature selection search and recording

Once features are selected and mapped from an image, the features are referred to as Pattern Tiles. They are selected by searching an image or an image subset, using the modified SEDA algorithm or by selecting a grid of points to be sampled.

2.1.3.1 SEDA method

The SEDA method starts by evaluating data from a 5 × 5 edge detection tile (edge tile) (Figure 2.5). When an edge tile meets the modified SEDA criteria, a pattern tile

maps an expanded area centered on the edge tile. The pixel values are rank ordered and compared with the mask values. If the high and low extreme mapped values are within the mask values, the pattern tile is stored, the counter is incremented and a *variable offset* is applied to allow spacing between the selected areas. The selection continues until the search area specified is exhausted. For this study, an 11 × 11 pattern tile was used.
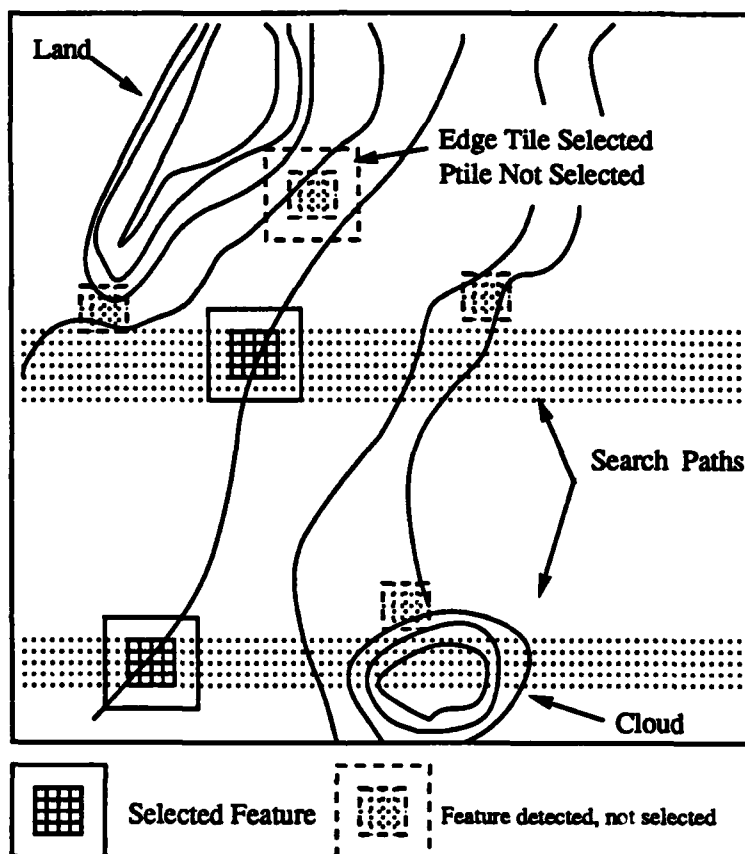
Figure 2.5: SEDA feature selection and discrimination. Selected tiles are on gradients in regions of moderate temperature change, free from clouds and land. Tiles not selected are rejected if the temperature in the mapped area exceeds classification criteria.

2.1.3.2 Grid search method

When regular spacing of points is desired, a grid pattern can be specified. Entering the coordinates of the pattern area, the program will sample an 11 × 11 tile at each point.

If the tile is acceptable, it is stored, the counter is incremented and the selection continues until the area is exhausted.

2.2 Feature tracking

2.2.1 Search area definition

Once the initial image has been processed and pattern tiles have been selected, the second image is used for feature tracking. The size of the area to be searched for each selected feature is governed essentially by the Bayes Decision rule [9]:

$$P(\theta \mid \vec{\zeta}) = \frac{P(\vec{\zeta} \mid \theta)P(\theta)}{P(\vec{\zeta})} \, , \qquad (2.3)$$

where $P(\theta \mid \vec{\zeta})$ is the *a posteriori* probability that an acceptable match will be found given an area to search defined by the vector $\vec{\zeta}$. The likelihood that an acceptable match can be found is expressed by:

$$\ell(\vec{\zeta}) = \frac{P_1(\vec{\zeta})}{P_2(\vec{\zeta})} \, , \qquad (2.4)$$

where $P_1(\vec{\zeta})$ is the probability that the feature is detectable, and lies in the search area. $P_2(\vec{\zeta})$ is the probability that the feature can be recognized and selected somewhere in the image. Equations 2.3 and 2.4 can be expressed as a maximum *a posteriori* probability (MAP) using the minus - log likelihood expression:

$$\frac{\partial}{\partial\theta}lnP(\theta \mid \vec{\zeta}) = \frac{\partial}{\partial\theta}lnP(\vec{\zeta} \mid \theta) + \frac{\partial}{\partial\theta}lnP(\theta) \, , \qquad (2.5)$$

where the first term on the right represents *a priori* information, and the second term is *a posteriori* information. Knowing that the selected features are altered over time by diffusion and rotation, and the displacement velocity varies greatly over short distances, equation 2.5 can only be solved through nonparametric density estimation. This is difficult, requiring *a posteriori* information. The estimate would certainly have large variances and bias values when completed. Having *a priori* knowledge of the maximum possible area (θ) the feature can move in during a sample interval, eliminates the need for nonparametric

methods. The problem simplifies to one of linear mapping and classification. Dropping the *a posteriori* term, subsequent searching is dependent on a Maximum Likelihood Estimation (MLE):

$$\frac{\partial lnP(\vec{\zeta} \mid \theta)}{\partial \theta} \mid_{\theta=\theta_{ml}} = 0 \ . \tag{2.6}$$

For a given set of sequential images, a notional area can be defined and centered in the succeeding frame using the coordinates of the selected pattern. The dimension of this area is defined by:

$$A_s = \pi \ R^2_{vmax} \ , \tag{2.7}$$

where A_s is the search area in pixels, and R_{vmax} is the maximum distance a feature could travel in one direction given its maximum expected velocity and the sampling period. R_{vmax} is determined by:

$$R_{vmax} = \frac{\nu_{max} \ t}{l_p} \ , \tag{2.8}$$

where ν_{max} is the maximum expected velocity of the feature in meters per second, t is the time in seconds, and l_p is the side dimension of the pixel in meters.
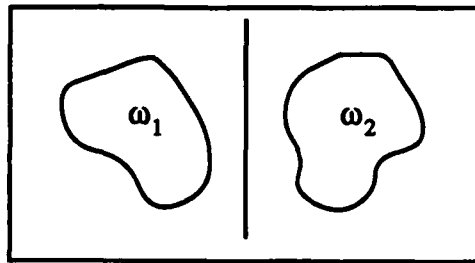
Figure 2.6: Ideal feature space mapping from pattern tile - search tile comparison.

When the search area is sampled, patterns will map into two feature spaces: a space where the minimum criteria are met, ω_1, and a space they do not, ω_2 (Figure 2.6). This sorting is accomplished using classifiers (Figure 2.7) to discriminate between groups. The criteria used in this work are the statistical correlation of the pattern tile - search tile pair, limiting the root mean square (RMS) temperature variation between the search and pattern tiles, and limiting the pattern and search tile inter-temperature ranges. Selection of the matching feature is made from the ω_1 space, picking the feature which best matches the pattern tile.
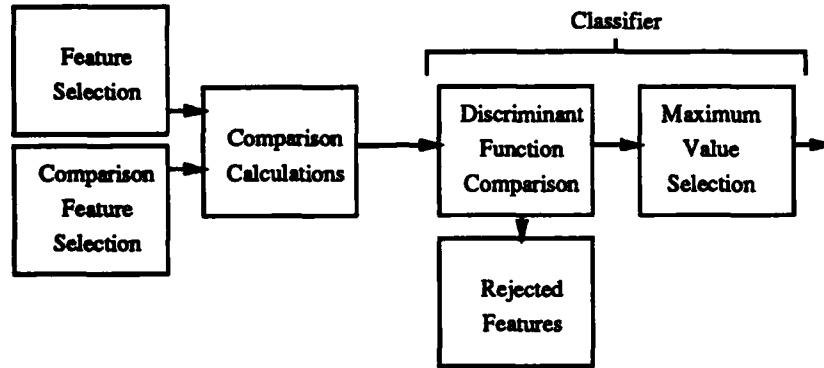
Figure 2.7: Search area pattern sorting and selection using classifiers.

Selection of the best match is a forward selection process of the members of the ω_1 space using a basic branch and bound procedure. The number of possible matches in a searched area, M, is defined by:

$$M = A_s - 1 .\tag{2.9}$$

The number of features which meet the classification criteria, $\bar{M}$, is determined by the number of features discarded during classification, $\bar{n}$, by:

$$\bar{M} = M - \bar{n} .\tag{2.10}$$

Final selection of the optimum feature $\bar{M}_{opt}$ assumes monotonicity of the samples, which allows the process to maximize the samples and pick the best feature such that:

$$\bar{M}_{opt} \geq \bar{M}_{\bar{M}-1} \geq \bar{M}_{\bar{M}-2} \cdots \geq \bar{M}_1 . \tag{2.11}$$

Maximum ocean surface current flow rates are known for most of the world, seldom exceeding one meter per second in the open ocean, and less than two meters per second for the Delaware Bay and estuary. Using the maximum likelihood - linear classification approach, search areas are limited to the region around each point which is most likely to contain the matching vector.

2.2.1.1 Search area dimension determination

The search area dimension is treated as a variable in this study. It is calculated for each image pair processed, depending on the following:

- Image pixel dimension.

- Time elapsed between images.

- Expected flow rate in the search area.

The image pair date time group is used to calculate elapsed time between images in seconds. This time is multiplied by the expected flow rate (meters per second) and the product is divided by the pixel dimension (1100 meters for this study) to generate the search radius vector. A notional square is calculated, using twice the search radius vector as its side dimension. This box is centered on the geographic center of the pattern tile, and the search is started (Figure 2.8).

2.2.2 Feature recognition and selection

2.2.2.1 Feature recognition

Search tiles are matched to pattern tiles using a common statistical correlation algorithm which has been constrained in a manner similar to SEDA algorithm. Statistical
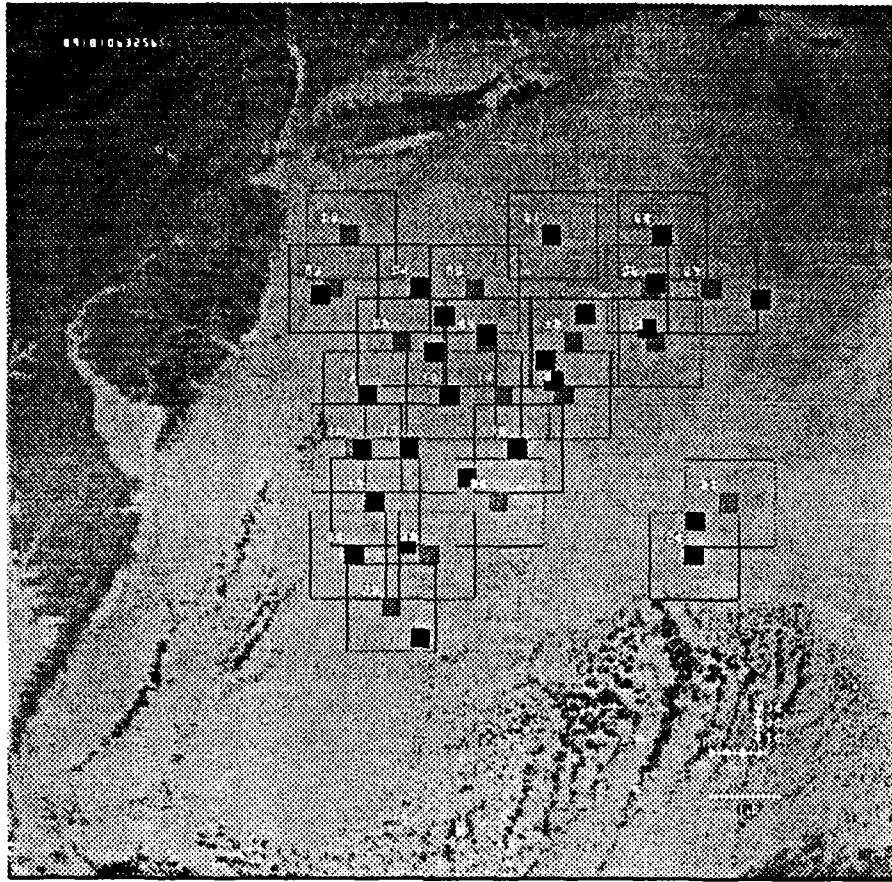
Figure 2.8: Search areas and best match selection, continental shelf region, 0132 hours local, 30 June 1989. Pattern tile positions are marked in blue, optimum match tiles are black.

correlation treats the pattern and search tiles as real, discrete, two - dimensional functions, $p(m,n)$ and $s(m,n)$. From Wahl and Simpson [3], the autocovariance and cross - covariance are given by:

$$C_{ss} = E[\{s(m,n) - \eta_s\}\{s(m + m_0, n + n_0) - \eta_s\}], \qquad (2.12)$$

$$C_{sp}(m_0, n_0) = E[\{s(m,n) - \eta_s\}\{p(m + m_0, n + n_0) - \eta_p\}], \qquad (2.13)$$

where $E[\cdot]$ is the expected value, (m_0, n_0) is the spatial lag between functions. η_s and η_p are given by the function means:

$$\eta_s = E[s(m,n)], \tag{2.14}$$

$$\eta_p = E[p(m,n)]. \tag{2.15}$$

The function variances σ_s^2 and σ_p^2 in fact are the zero - lag autocovariances. This allows the correlation coefficient to be defined as:

$$r_{sp}(m_0, n_0) = \frac{C_{sp}(m_0, n_0)}{\sigma_s \sigma_p}, \tag{2.16}$$

such that $\|r_{sp}(m_0, n_0)\| \leq 1$ and $r_{ss}(0,0) = 1$. This means that if a chosen search tile is an exact spatially dislocated version of the first signal, then:

$$s(m,n) = p(m + m_0, n + n_0), \tag{2.17}$$

and $r_{sp}(m_0, n_0)$ must equal one. In matrix form, the correlation coefficient can be calculated using the following:

$$r_{sp}(k,l) = \frac{\sum_i \sum_j [s(i+k, j+l) - \eta_s(k,l)][p(i,j) - \eta_p]}{\left[\sum_i \sum_j [s(i+k, j+l) - \eta_s(k,l)]^2 \sum_i \sum_j [p(i,j) - \eta_p]^2\right]^{\frac{1}{2}}}. \tag{2.18}$$

Applying tile correlation in this manner estimates the image spectrum in an autoregressive manner [10]. The advantage in using this method as a selection criteria is that it is less sensitive to background noise. Use of the correlation method to select matching features is well accepted and is widely used. While computationally intensive, for pattern

tiles 12 × 12 and smaller, it has been proven that calculating the correlation directly is faster than using either discrete or fast fourier transformation techniques [3].

2.2.2.2 Feature rotation

Given time periods between images of 12 - 24 hours, it is almost certain that ocean thermal features are *rotating* as well as displacing in the X - Y plane. This is especially true in eddy flow areas such as the one observed over the continental shelf, south of Long Island. Methods exist [11] to transform the pattern tile to different axis orientations. A single rotation transformation to allow for a left or right movement would increase computations by a factor of three. Rotation transformations are not calculated in this program to speed execution time.

Emery [12] states that a correlation above 0.4 is has a 99% significance for features that have rotated in the X - Y plane as much as 40 degrees. Wahl and Simpson [3] recommend correlations of 0.65 or greater. This study uses a minimum coefficient of $r_{sp} = 0.60$.

2.2.2.3 Feature selection

To reduce the number of calculations performed, a tile with dimensions equal to the edge detection tile is first moved through the search area. A correlation between this tile and the center of the pattern tile is made and compared to a threshold. If the desired value is met, the full search tile area is remapped around the center of the smaller tile.

The search tile area is then correlated with the full pattern tile. If the correlation criteria is met, the root mean square (RMS) difference of the tiles is evaluated to insure that the mean temperature change of the tile does not exceed a physically realistic maximum. This limit is typically in the range of 3 - 5° C (24 - 40 pixel counts). Additionally, the highest and lowest ranked pixels are also compared to the temperature thresholds.

These error checks are required because the correlation coefficient is affected by spatial dislocation in three dimensions, not just two (Figures 2.9, 2.10 and 2.11). A search tile that is an exact match for the pattern tile in the X and Y dimensions, can also vary in the Z, or temperature dimension, as well. A *uniform change* in temperature
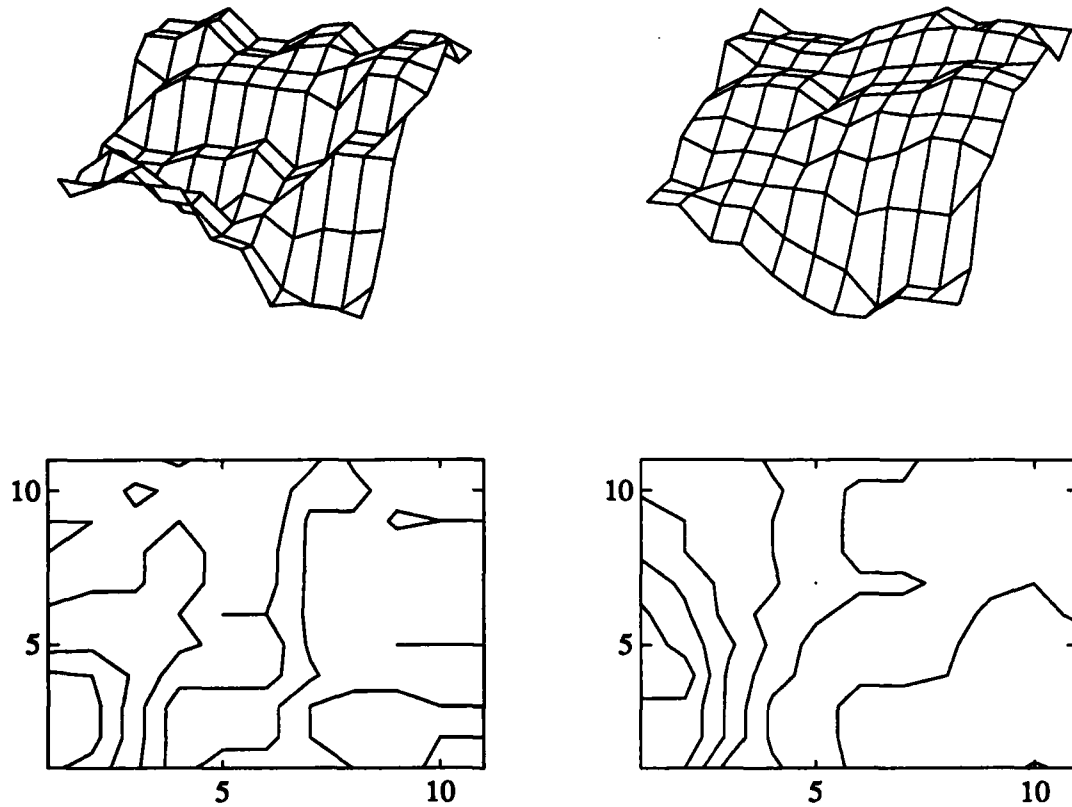
Figure 2.9: Pattern tile - search tile correlation: $r_{sp} = 0.85$.

can yield a high correlation, but give an erroneous selection. This occurs most commonly over land and water in the presence of light or scattered clouds. Light clouds may differ in signal by 30 pixel counts or less from a water surface.

As the program finds features that meet the threshold criteria, they are compared to the currently stored value. If the feature has a higher correlation, it overwrites the previous entry and increments a counter. When the search area is exhausted, the area with the highest correlation to the pattern tile is used to compute the surface flow.
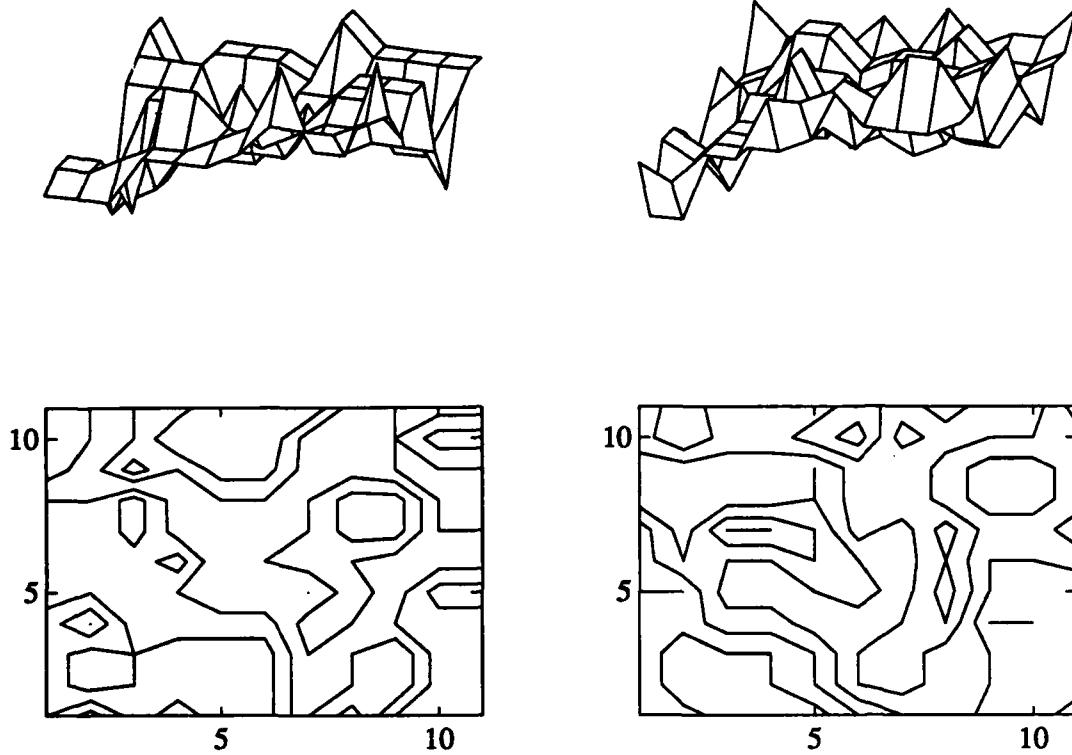
Figure 2.10: Pattern tile - search tile correlation: $r_{sp} = 0.63$.

2.3 Direction and magnitude computation

Once search tile selections have been made, the x and y values are compared for each tile pair. Trigonometric calculations are performed to determine vector length (magnitude), direction (azimuth) and flow rate in meters per second. To improve computational speed, the calculations are switched to specific routines based on the difference of the tile locations.

The magnitude of the vector is computed the expression:

$$l = \sqrt{(x_0 - x_1)^2 + (y_0 - y_1)^2} \,. \tag{2.19}$$

The direction is found using:
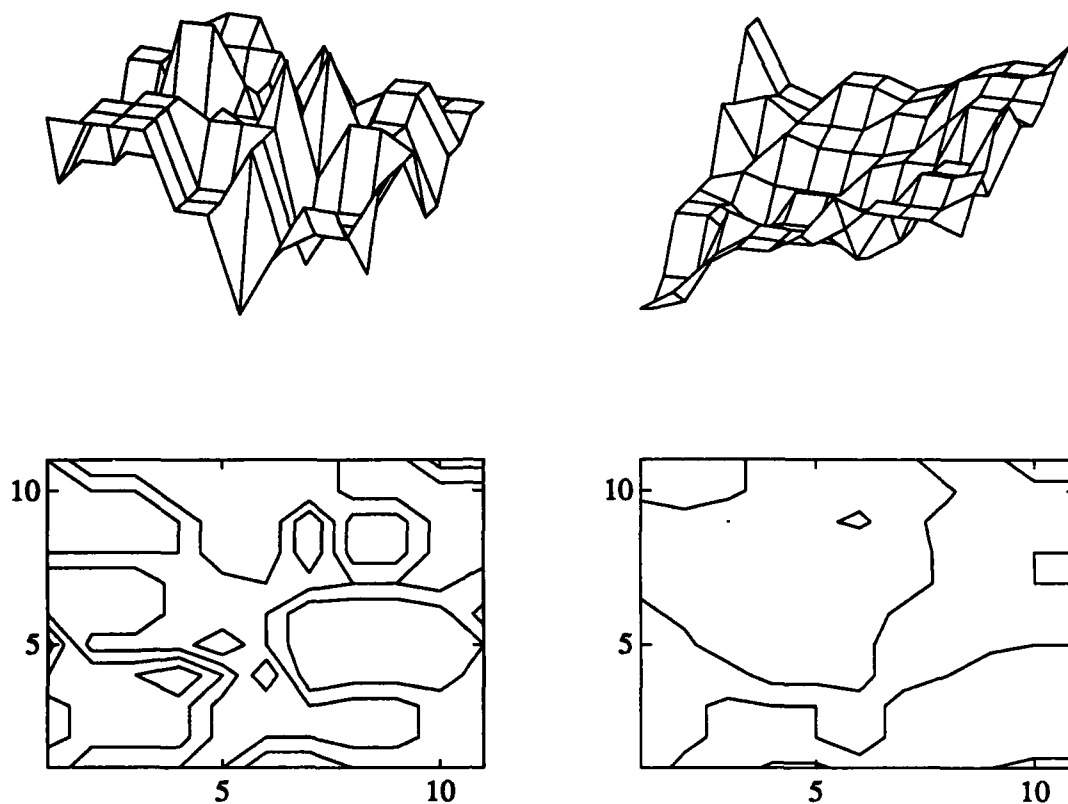
Figure 2.11: Pattern tile - search tile correlation: $r_{sp} = 0.25$.

$$\theta = \arccos \frac{hsum}{l} . \qquad (2.20)$$

θ is then converted to azimuth based on the quadrant in which the angle was computed.

Trigonometric transformations for arrowheads are also made in these subroutines, using the expression:

$$P_{2(arrow)} = \left(X_{P_{2(line)}} \pm \cos \theta^1 \times M\right) \pm \left(Y_{P_{2(line)}} \pm \sin \theta^1 \times M\right), \qquad (2.21)$$

where θ^1 is the angle of the arrow head from the line, and M is the arrowhead length.

The vector lines and arrowheads are drawn on the image using a C-language version of Bresssenham's integer line drawing algorithm [13].

2.4 Cloud detection

The ability of the SEDA and constrained correlation methods to operate with images that contain land and clouds is a significant advantage (Figure 2.12). Of more than 131 images reviewed from the period 1 March to 30 June 1989, only 6 sets were sufficiently open in the area of interest to permit study.
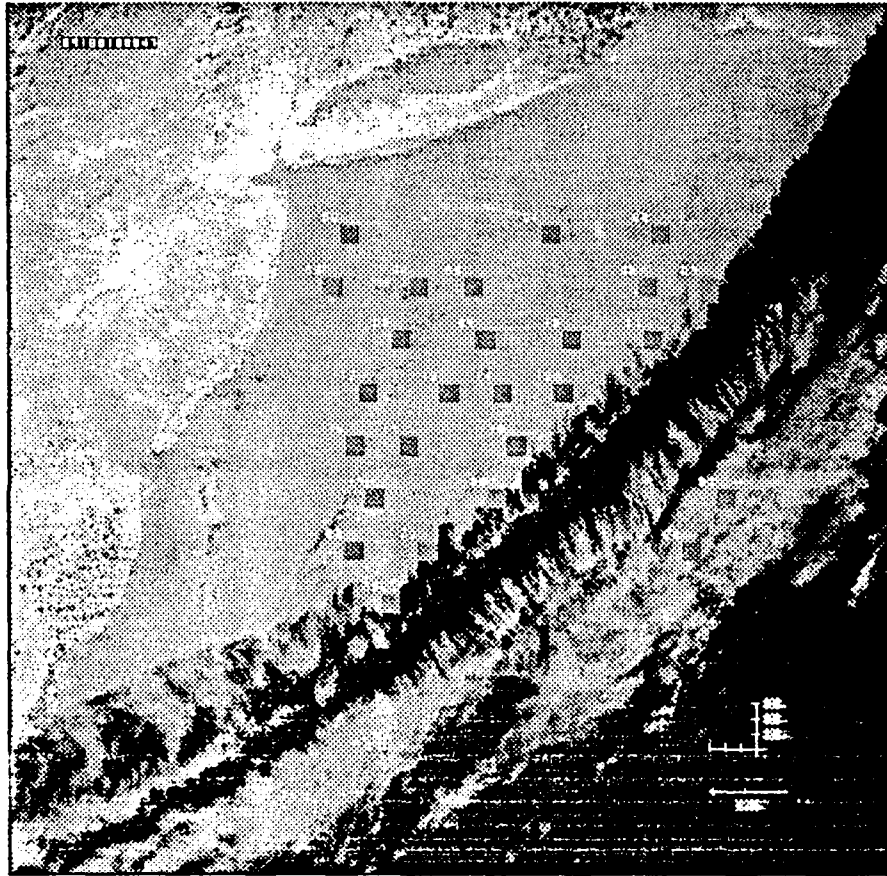
Figure 2.12: Pattern tile selection in cloudy conditions, continental shelf region. 1308 hours local, 29June 1989.

However, the SEDA method is not adequate as a method for screening images in an automated manner. Uniformly thin cloud layers can defeat the method, producing a

large number of false vectors. To screen large numbers of images, a more effective cloud screening method such as Simpson's [14] or Gautier's [15] is recommended.

Chapter 3

SURFACE FLOW IN THE DELAWARE COASTAL REGION

3.1 Area studied

This project observed the surface thermal feature displacement in two areas: the Delaware coastal region, and an area of interesting eddy flow over the continental shelf, south of Long Island. Comparison to *in situ* anchored buoy data has been made for the Delaware coastal region.

Images used for this study are listed in table 3.1 by their date time group (DTG). The DTG is can be read as follows:

$$\text{Example DTG: } 89181063256$$
$$yy\ ddd\ hh\ mm\ ss$$

where yy is the year (89 = 1989), ddd is the julian date, hh is the hour in Greenwich Mean Time (GMT), mm are the minutes and ss are the seconds.

3.2 Analysis of surface flow in the Delaware coastal region

The flow of surface, subsurface and bottom currents in the Delaware coastal region has been extensively studied. A recent report by Münchow [16], provides an excellent presentation of this information. Figure 3.1 shows approximate locations for 21 of 31 anchored buoys used in his study. These buoys have mean observations for current velocity and direction for depths between 5 and 10 meters. Satellite observations in the coastal area have been correlated with these observations as listed in Table 3.2.

30

Table 3.1: NOAA satellite images used in this study, listed by date time group.

NOAA Images Used	
Period	Image DTG
10-11 March 1989	89069170021
	89069184155
	89070183134
28-29 May 1989	89148071223
	89148165803
	89149070111
10-12 June 1989	89161063805
	89161180325
	89162062806
	89163061744
	89163080102
29-30 June 1989	89180180847
	89181063256
	89181175808

3.2.1 Observations 10 March - 30 June 1989

3.2.1.1 10-11 March

Figure 3.2 shows that thermal features are detected in the coastal region. The program performs well in selecting only water features. However, no search tiles were selected for either image pair from this period.

The output data shows that the sea surface temperature (SST) and bay temperature is very low, $5.25°$ to $5.62°$ C respectively. This represents a range from 26 to 61 in pixel values. Of the 31 pattern tiles selected, 16 found no reduced set search tiles that met the correlation criteria. The remaining 15 computed from 79 to 137 full tiles, but none had an $r_{sp} > .50$.

The low correlation suggests a very deep mixed layer due to the cold water temperature at the surface. This means that the vertical diffusion condition ($\frac{\partial T}{\partial z} \ll \frac{\partial T}{\partial x}$) is not met due to continuous vertical mixing of surface and deep (greater than 50 meters) water [17].

Table 3.2: Selected anchored buoy near surface current measurements (from Münchow).

M_2 tidal properties			
Mooring	Depth (meters)	Axis degrees	Velocity cm/s
1	4	127	94.3 ± 0.3
2	4	123	80.2 ± 0.1
3	6	126	60.8 ± 0.2
4	5	139	43.5 ± 0.1
5	5	137	69.6 ± 0.1
6	5	120	24.1 ± 0.4
7	5	148	21.0 ± 0.1
8	5	160	18.7 ± 0.3
9	5	160	16.5 ± 0.2
11	6	106	17.6 ± 0.2
12	3	129	24.2 ± 0.2
14	6	152	25.1 ± 0.0
16	6	97	17.2 ± 0.3
17	6	97	16.8 ± 0.4
18	6	111	19.9 ± 0.3
19	6	202	7.1 ± 0.3
20	6	187	8.2 ± 0.4
21	6	179	10.8 ± 0.4
22	8	150	21.6 ± 0.2
24	7	157	7.7 ± 0.2
25	8	144	9.4 ± 0.3
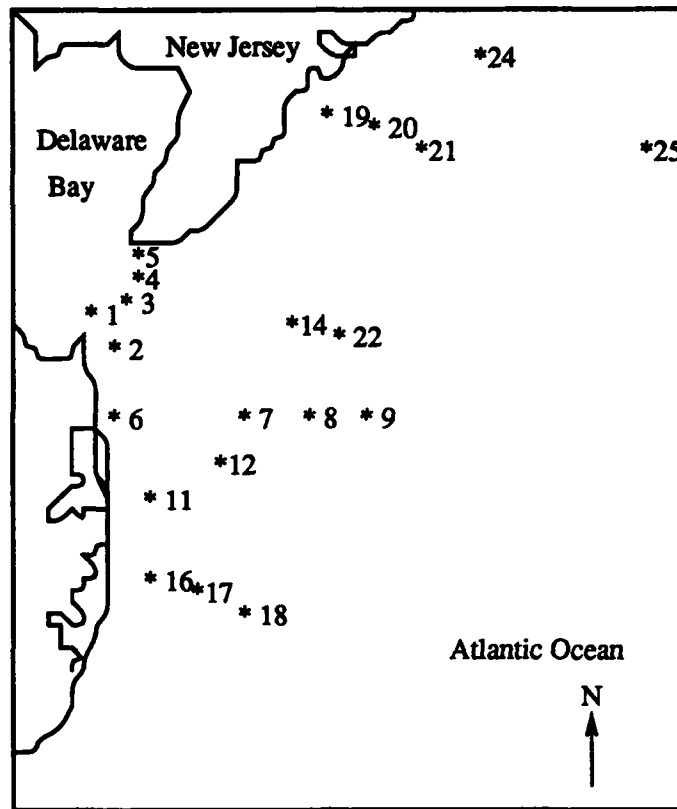
Figure 3.1: Selected anchored buoy locations for the Delaware coastal region, which were used to evaluate accuracy of satellite derived surface current flow.

3.2.1.2 28-29 May 1989

Figure 3.3 shows magnitude and direction vectors for a 12 hour, 3 minute period, 28 May 1989. The three images available were processed as two pairs. Only the pair 89148165803 to 89149070111 were acceptably cloud free to observe the Delaware coastal region, producing 22 pattern tiles and 10 vectors.

The continental shelf area was observed using the grid technique for both days. In each case, 49 pattern tiles were selected, with only 10 search tile selections for the period from 07-1600 GMT, and 16 selections for the 16-0700 GMT period. The small selection rate is attributed to a combination of vertical mixing due to low water temperature (15.5° C in the bay, 12.6° C offshore) and rotation of features in the eddy areas.
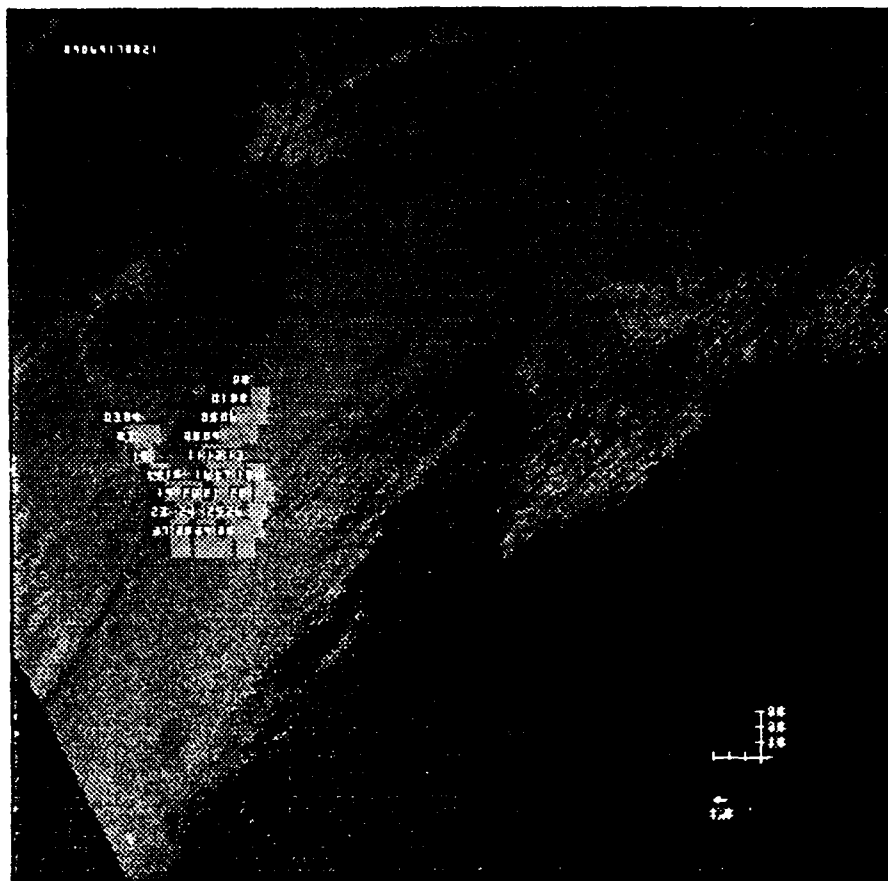
Figure 3.2: Pattern tile selection in the Delaware Bay and coastal region. 1100 hours local, 10 March 1989.

3.2.1.3 10 -12 June 1989

Figure 3.4 shows a high density sampling of the flow around the Delaware coastal region, 12 June 1989. Four images were available for analysis, including one pair with a 24 hour spacing and another pair with a 2 hour interval. In four comparisons, 94 vectors were produced from a pattern tile set of 142. This increase in selection shows stratification has occurred and a surface mixed layer has formed and is more stable with water temperatures reaching 18.63° C in the bay and 16.13° C offshore.

The continental shelf area was evaluated using both grid and SEDA methods. 93 out of 187 pattern tiles selected produced vectors. The flow pattern was not well defined in this set, but is similar to the flow defined in Figure 3.6.
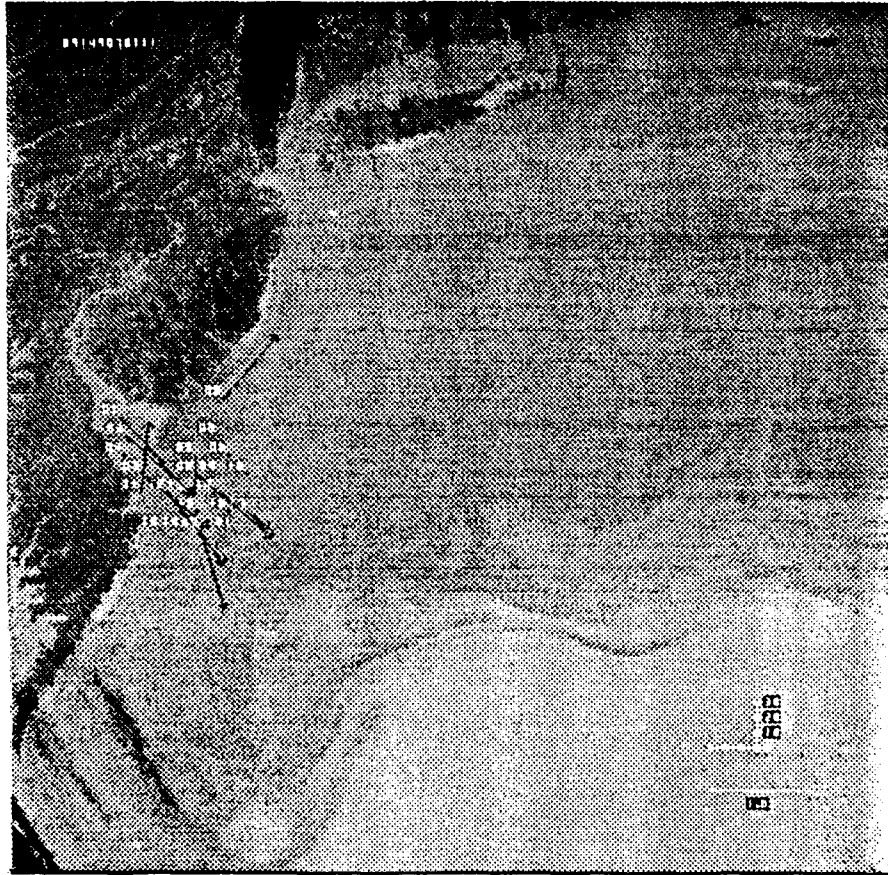
Figure 3.3: Labeled flow vectors in the Delaware Bay and coastal region for a 12 hour period ending 0201 hours, 28 May 1989.
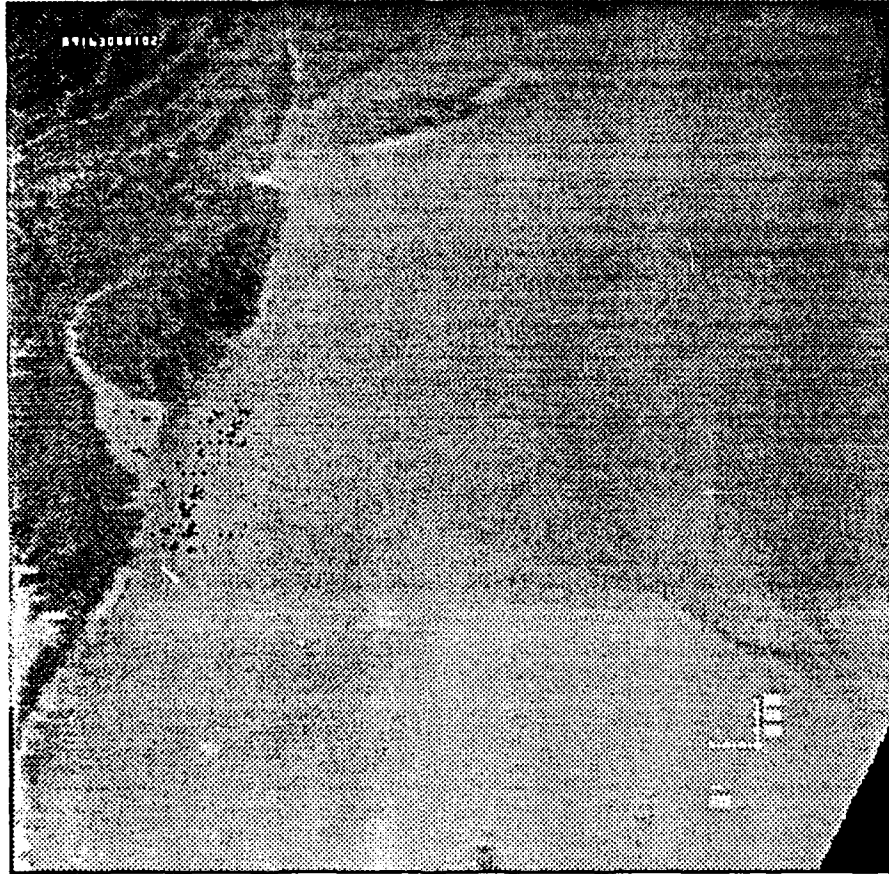
Figure 3.4: High density flow vectors in the Delaware coastal region, for a 2 hour, 16 minute period ending 0201 hours local, 12 June 1989.
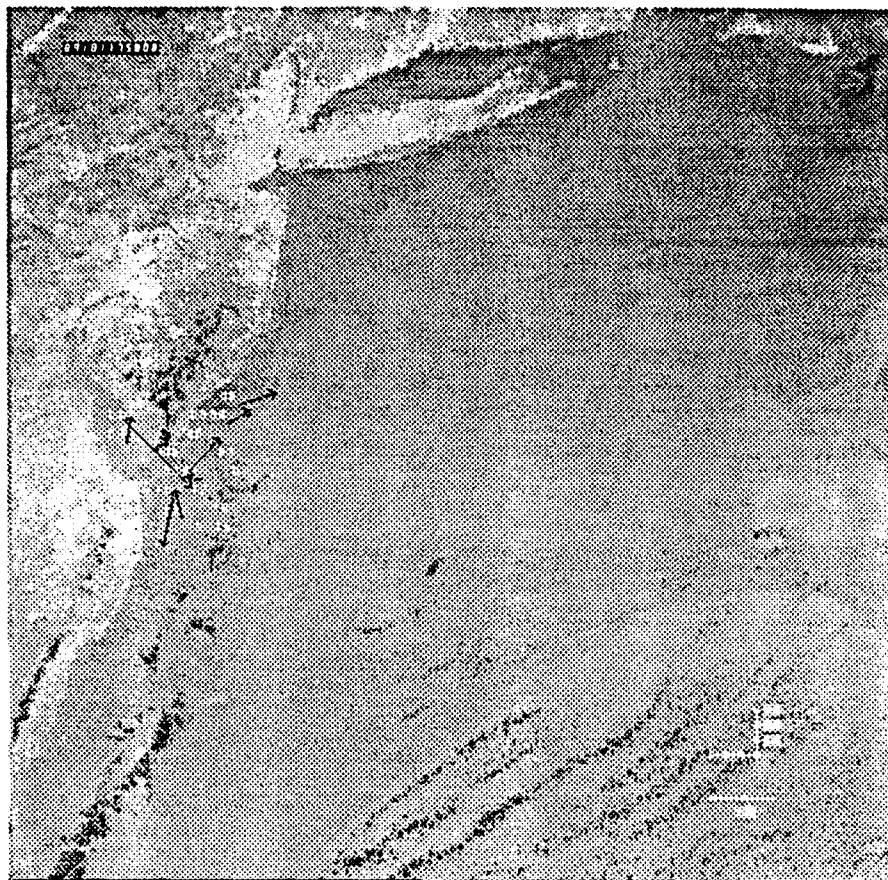
Figure 3.5: Surface flow vectors in the Delaware coastal region, for an 11 hour, 28 minute period ending 1258 hours local, 30 June 1989.

3.2.1.4   29-30 June 1989

Figure 3.5 shows general surface flow in the Delaware coastal region, 30 June 1989. Three images were available for this period. Each was spaced by approximately 12 hours, and were processed as two pairs. 105 vectors were obtained from 171 pattern tiles. Search tile matching was hampered by light clouds which moved into the offshore region in each comparison image. Sea Surface temperature was very warm, measured at 21.38° C for the bay, and 20.5° C for the offshore area.

The continental shelf region was evaluated using both the SEDA and grid methods. Figure 3.6 shows 53 vectors derived from 110 pattern tiles. Feature rotation is the most probable cause for the low selection rate. Horizontal and vertical diffusion are certainly a
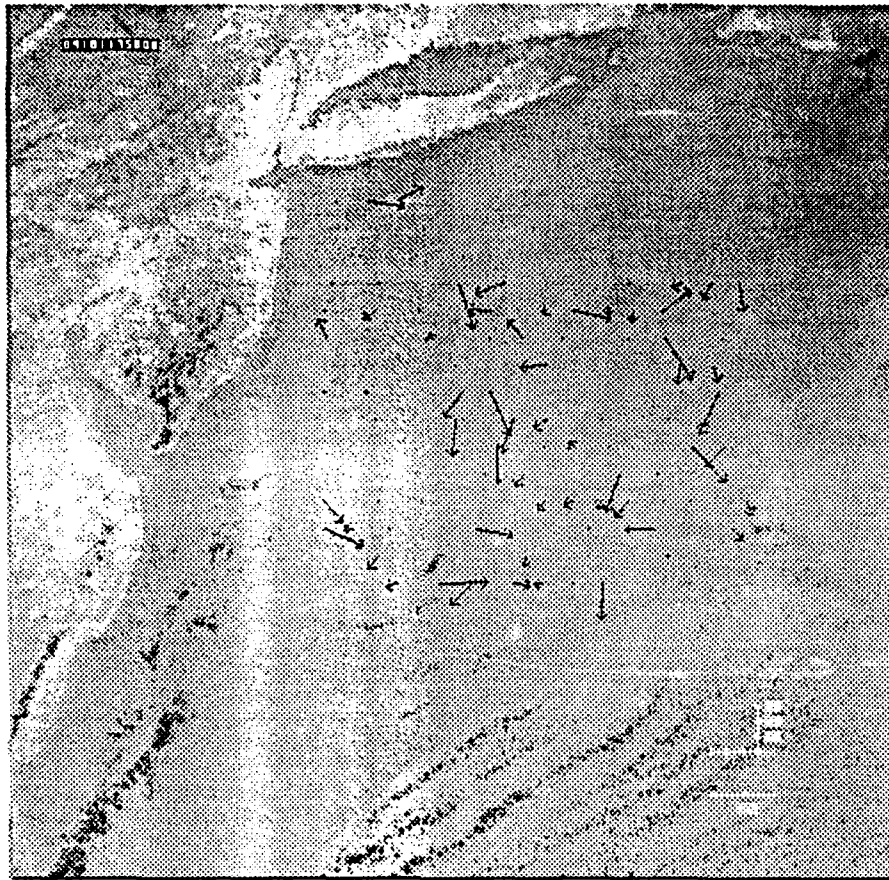
Figure 3.6: Surface flow vectors in the continental shelf region, for an 11 hour, 26 minute period ending 1258 hours local, 30 June 1989.

factor in the eddy regions.

3.2.2 Comparison of satellite observations and buoy data

Verification of this program to accurately measure displacement of surface thermal features, and judge the validity of using this movement to infer actual near surface currents, was accomplished by comparing program derived vectors with *in situ* buoy data. 110 vectors were matched to 17 buoy positions. The mean of these values for each station was derived (Table 3.3), and the results were correlated with good results (Table 3.4).

These values were obtained by computing the mean of vectors obtained by visually matching program vectors with the closest buoy station. Vectors were rejected if the

Table 3.3: Mean satellite observations for selected *in situ* buoys from Table 3.2 Values were determined by matching satellite derived vector origins with buoy positions. The values listed are the means of multiple observations for each location.

Mean satellite - buoy observations		
Mooring	Axis degrees	Velocity cm/s
1	131.02	112.80
4	134.37	36.75
5	159.86	79.00
6	116.45	34.00
7	90.00	27.0
9	174.34	12.50
11	108.43	42.00
12	165.85	26.00
14	180.19	32.33
16	92.33	26.00
17	111.07	27.00
18	117.96	23.67
19	217.46	12.50
20	193.28	18.50
21	168.74	16.40
22	146.48	40.00
24	164.52	10.50

Table 3.4: Satellite - Buoy azimuth and velocity comparison.

Mean satellite - buoy comparison	
Parameter	Result
Azimuth Correlation	.83
Std. Deviation (σ_{Az})	20.45°
Mean Error	-4.38°
Velocity Correlation	.96
Std. Deviation (σ_V)	7.76 cm/s
Mean Error	-7.75 cm/s

magnitude or direction were obviously false (velocity errors greater than a factor of 3, or more than 60° off in azimuth), due to cloud or land contamination (see vector 11, Figure 3.3), prior to determining the mean value. Vectors with direction errors of $180^\circ \pm 60^\circ$ were considered to be on the flow axis and were converted by adding or subtracting 180° as appropriate. Of the 110 vectors considered, 27 were rejected using this criteria, giving a final sample size of 83.

The agreement in velocity between the satellite and buoy measurements is particularly good with a σ_V of only 7.76 cm/s over a range from 9 to 112 cm/s. The azimuth correlation is also a good match. The σ_{Az} of 20.45° reflects the small sample size, and would decrease with more data points.

3.2.3   Comparison with the Simpson Minimum Distortion Log Search method

A program using the Simpson Minimum Distortion Log Search Method [6] is available on line in the University of Delaware Center for Remote Sensing. In its current form only the two images from the 30 June 1981 period are available for comparison, using a 40×40 pixel grid in the continental shelf region. This program was run in the grid mode producing 13 vectors from 49 pattern tiles selected. The correlations for these methods is very low: .31 in velocity, and .23 in azimuth.

The most probable reasons for these low correlations are a differing of search area dimensions (this program searches an area four times larger than the Simpson method), and the difference in search tile selection methods. The Simpson program forces selection of a vector for each pattern tile in the area which shows the least distortion. This program is more stringent, requiring a statistical correlation, rejecting features which do not meet desired criteria.

Chapter 4

CONCLUSION

4.1 Summary

This program is a tool which can be used to estimate surface and near surface currents, by objectively measuring the displacement of large water surface thermal features. It utilizes commonly available satellite images with no special enhancement or processing requirements. The constrained Ordered Statistical Edge Detection algorithm employed to select features is capable of discriminating between desired water surface features and other background objects such clouds or land. The program is written in the C computer programming language, and has been run on a variety of common systems including:

- Silicon Graphics - Personal Iris.

- Digital Equipment Corporation - DEC Station 5000.

- Sun Microsystems - Sun-3 operating system.

The program produces output in image and text form. Images are labeled with identification numbers to allow comparison of the text file and the output images.

The high correlation values derived from comparing satellite image derived measurements with *in situ* buoy data, combined with the ability to use images which have clouds and land present, make this program a good tool for the study of coastal and open ocean waters. Results generated by this program will provide useful input for mixed layer depth modeling [18].

4.2 Acknowledgments

the United States Army, under the provisions of Army Regulation 621-1, and the Fully Funded Advanced Civil Studies program.

Appendix A

COMPUTER PROGRAM DESIGN

The computer program which generated the data and images used in this work has an operating system consisting of seven major sub-groupings:

- Program Setup and User Interface.

- Image Input.

- Pattern Tile selection.

- Search Tile / Pattern Tile matching.

- Surface Flow Computation.

- Image Graphics.

- Output.

Program operation is illustrated in figure A.1.

A.1 Program setup and user interface

Program initialization, setup and user interface are provided by the following routines:

- main.c.

- setup.c.

- userinput.c.

43
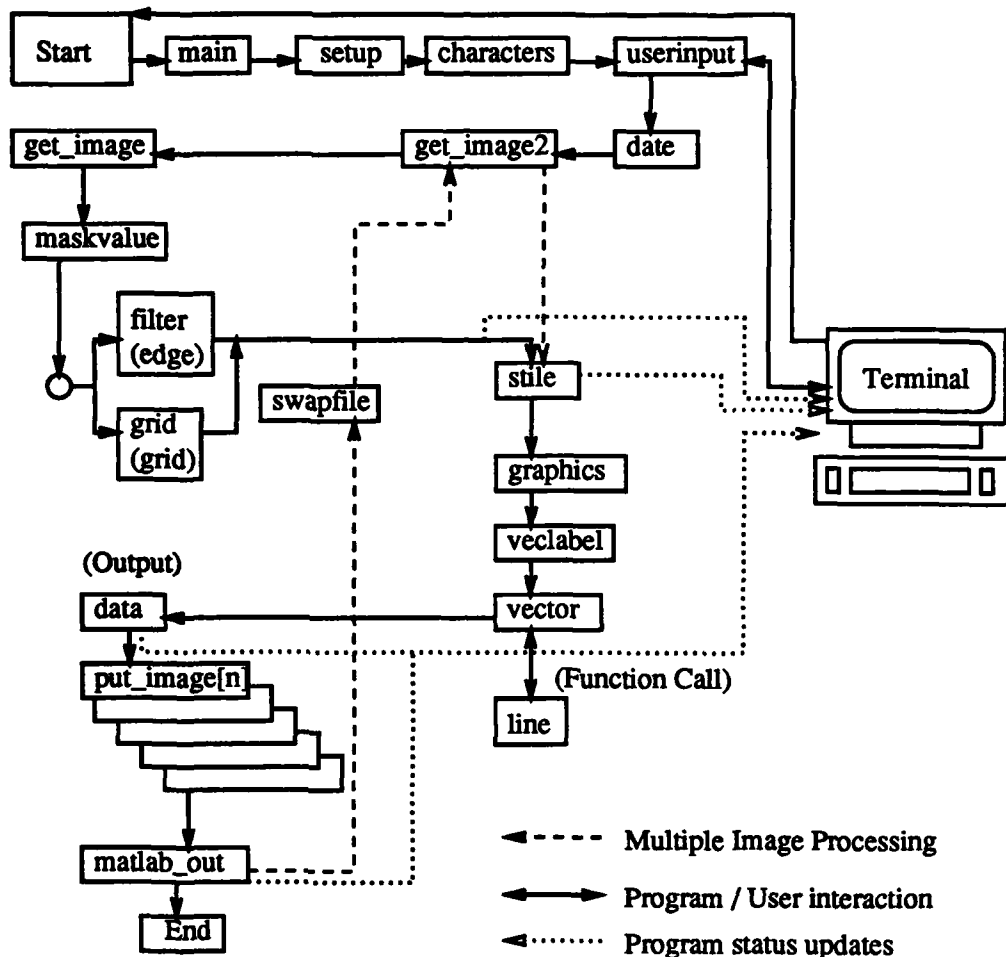
Figure A.1: Ocean flow estimation program flow chart.

- date.c.

- characters.c.

- image.h.

Main.c is a standard C routine which defines the computer program flow chart. Setup.c contains the default values for the program global variables. Userinput.c produces a series of screen menus and prompts to allow single run changes to the program parameters. Date.c strips the date time groups from the command line starting the program to compute elapsed time. Characters.c contains the character bit map for graphic

labels placed on the processed images. Image.h is a header file which contains structure variable and global function and value declarations.

A.2 Input / Output functions

Image input and output for this program are fairly standard routines that are in common use. The input functions are found in;

- get image.c.

- get image2.c.

Input images may be processed without headers or in the Interactive Viewing and Analysis System (IVAS) [19] format, concatenated with a four line header.

Output images can be output with or with the header by changing commenting around the header write commands in the output files. Headers must be removed when using Ximage or similar non-IVAS compatible viewing tools. Image output is performed in these files:

- put image.c.

- put image2.c.

- put image3.c.

- put image4.c.

- put image5.c.

Text files are generated at the end of computations from the routines:

- data.c.

- matlab out.c.

This output can be customized to meet user needs. Current output goes to two files:

- flowdata[n].

- matdata[n].

flowdata[n] is a text file that lists results of each run (see Appendix D). The counter [n] is incremented when multiple images are processed to provide the data from each image pair comparison. *matdata*[n] is a matrix output of the pattern tile - search tile pairs in PRO - MATLAB format [20].

Userinput.c is a routine which allows the user to make one time changes to the program parameters. This routine also prompts the user for setup information which may frequently change. Shown below is an example of the user screen if all options are reviewed and changed.

```
> flow 1 89069170021 89069184155
Are the image dimensions (Xdim) 512 X 512 (Ydim)? (y/n) :y
Do you want to view default setup ? (y/n): y

Changes are made for this session only, changes in
         default values are made by editing 'setup.c'

Area of Interest: xmin-40 ymin-210 , xmax-160 ymax-300

Pattern tile Default selection criteria:
         Search Option:               edge
         Tile size :                  11
         Edge detect tile size:        5
         Ptile minimum offset:        20
         Filter minimum edge threshold:   6
         Pixel difference value range:   12

Search tile Default selection criteria:
         Search area flow rate:     0.50
         Stile search increment:       1
         Allowed velocity error:    0.20
         Allowed Temperature error: 4.00
         Allowed variance from mean:2.00
         Minimum correlation value: 0.60

Changes can be made by entering:

  a -(area of interest) p -(ptile) s -(stile) d -(done):a
```

```
Enter search area xmin: 40
Enter search area ymin: 210
Enter search area xmax: 160
Enter search area ymax: 300

Enter a to re-edit, p -ptile, s -stile, or d -done:p


Enter Search option (1=Edge Detection, 2=Grid Search): 1
Enter Ptile/Stile size number(Larger than Edge & odd; 5,7,9,11): 11
Enter Edge Detect tile size (should be odd; 3,5,7...): 5
Enter Ptile minimum offset: 20
Enter filter minimum edge threshold: 6
Enter pixel difference value range: 12

Enter p to re-edit, a -area of int, s -stile, or d -done:s


Enter search area flow rate: .5
Enter Stile search increment: 1
Enter allowed Tile RMS temp. difference ( deg. C): 4
Enter minimum correlation value (0.1 - 1.0, usually 0.6): .6

Enter s to re-edit, a -area of int p -ptile, or d -done:d


Search Area = 4, for a max flow rate of 0.5

Do the input images have headers? (y/n):n
Do you want the output images to have headers? (y/n):n

Min mask value: 26, Max mask value: 61, Del bay: 45 (5 C), Coast: 42 (5 C)

Ptiledata start
ptiledata complete 10 ptiles
starting stile.c
finished with stile.c
writing boxes onto st image
writing stiles to image
Starting vector.c
Output is going to flowdata1
Output is going to matdata1.m
>
```

A.3   Pattern tile selection

Pattern tiles are selected in the file:

- filter.c (ordered statistic edge detection).

- grid.c (Specified x - y placement).

Pattern tile dimensions are variable. For this study a 5 × 5 array (25 subtiles) was used to detect features, an 11 × 11 tile mapped features that were selected. The values for the feature discrimination values $mask_1$ and $mask_2$ are calculated in the routine:

- maskvalue.c

Masks can be placed anywhere on an image depending on user needs. For this study, masks were placed in the Delaware bay and 40 kilometers off shore from Cape May, New Jersey. The masks are computed from tiles the same size as the mapped pattern tile.

A.4 Search tile operations

Search tile correlation and selection take place in the file:

- stile.c.

A.4.1 Correlation coefficient and RMS difference computation

To reduce the amount of dynamic memory required, only search tiles that meet the classification criteria are stored temporarily in a two dimensional structure. If a search tile fails to meet correlation or RMS difference criteria, it is not stored and the count is not advanced. Additionally if the correlation value is not greater than the previously recorded matched tile, the tile is not recorded and the count is not advanced. This means that when the search tile box has been exhausted, the closest match is at the top of the structure and is recorded for vector calculation.

Using a reduced set search (5 × 5 versus 11 × 11) reduces the total number of calculations by roughly a factor of four. A 30 × 30 search box using a 5 × 5 search tile has 625 iterations of 25 calculations each (15,625 calculations). Searching with an 11 × 11 tile would take 75,625 calculations. The actual total lies somewhere in between. Table A.1, shows numbers from a typical run. The small number of times that the full tile was computed produced a factor of four improvement in execution speed.

If no search tile meets either of the threshold criteria, the pattern tile location values are recorded for the search tile and no flow magnitude or direction is calculated.

Table A.1: Reduced set search calculation savings

Search Box Dimension 47 × 47				
2209 iterations per tile				
Tiles Selected	Full Tiles Computed	Cost all 11 × 11	Cost this run	Savings this run
15	473	4,009,335	940,833	76.54 %

A.5 Vector magnitude and direction calculation

Vector operations are performed in the file:

- vector.c.

Once search tile selections have been made, the x and y values are compared for each p-tile - s-tile pair. Trigonometric calculations are performed to determine vector length (magnitude), direction (azimuth) and flow rate in meters per second. To improve computational speed, the calculations are switched to specific routines based on the difference of the p-tile and s-tile locations:

$$hsum = s - tile(x) - p - tile(x),$$

$$vsum = s - tile(y) - p - tile(y).$$

Magnitude of the vector is computed the expression:

$$l = \sqrt{hsum^2 + lsum^2}.$$

Direction is found using:

$$\theta = \arccos \frac{hsum}{l}.$$

θ is converted to azimuth based on the quadrant for with the angle was computed (figure A.2).
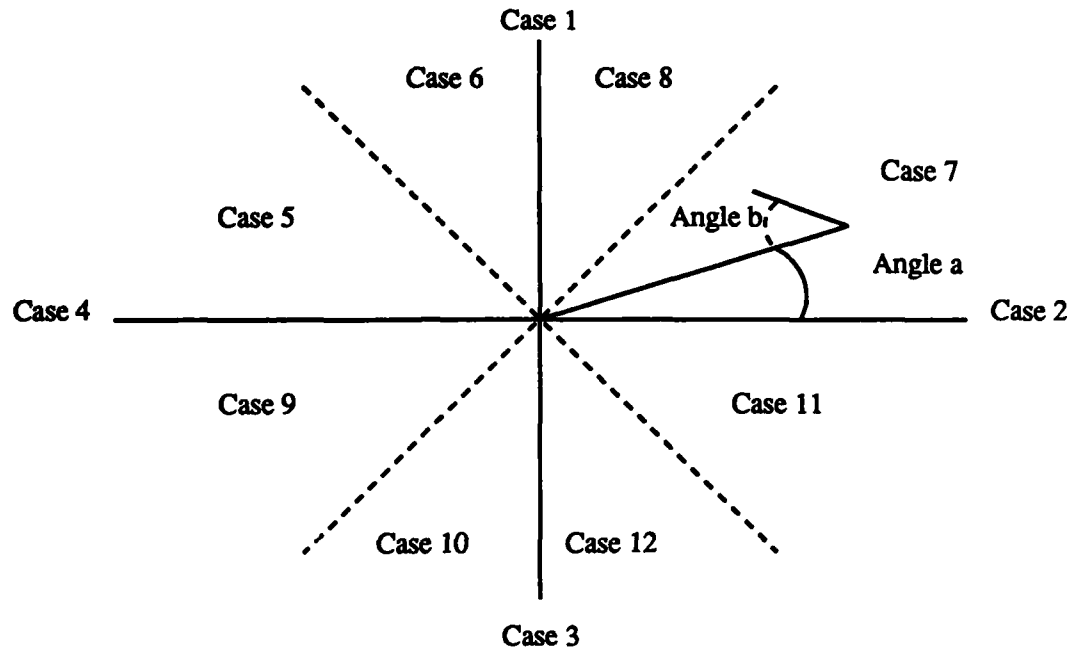
Figure A.2: Vector transformation diagram used to calculate vector azimuth and end points for arrowheads

Trigonometric transformations for arrowheads are also made in these subroutines, using the expression:

$$P_{2(arrow)} = (X_{P_{2(line)}} \pm \cos\theta^1 \times M) \pm (Y_{P_{2(line)}} \pm \sin\theta^1 \times M),$$

where θ^1 is the angle of the arrow head from the line, and M is the arrowhead length.

The vector lines and arrowheads are drawn on the image using a C-language version of Bresssenham's integer line drawing algorithm [13] which is found in the routine:

- line.c.

A.6 Program validation

To check the program to insure that it is properly mapping and calculating pattern and search tiles, the program was run using the same image for tile selection and comparison. This was accomplished by copying the image and altering its date time group by 12

hours. The program was executed normally with the desired result being the search tile selection of the pattern tile. Correlations (r_{sp}) of 1.00, changes in temperature of 0.0, and 0.0 values for all vector calculations indicate a working program. A program test in the Delaware coastal region is shown below:

```
From: 89181063256,  To: 89181180000:
Elapsed time:  0 Day(s), Total: 12 Hours, 32 Minutes, 56 Seconds
Search box dim:51 Offset: 20 Tile dim: 11 X 11 Number of samples 9
pt lngth(km) az(deg) flow m/s
  0   0.00      0.00    0.00
  1   0.00      0.00    0.00
  2   0.00      0.00    0.00
  3   0.00      0.00    0.00
  4   0.00      0.00    0.00
  5   0.00      0.00    0.00
  6   0.00      0.00    0.00
  7   0.00      0.00    0.00
  8   0.00      0.00    0.00
Average flow distance: 0.00 km, Avg Az: 0.00 deg, Avg flow rate: 0.00 m/s
```

```
Search tile data (x,y coord for center subtile)
ptile stile  x    y  CC val Pt temp St temp del T Pt sum St sum Ratio
  0   116   69  241  1.00   22.55  22.55  0.00  21826 21826 1.00
  1    57  129  241  1.00   21.07  21.07  0.00  20393 20393 1.00
  2   145   75  262  1.00   20.71  20.71  0.00  20044 20044 1.00
  3    32  109  262  1.00   20.64  20.64  0.00  19982 19982 1.00
  4    29  133  262  1.00   21.57  21.57  0.00  20877 20877 1.00
  5   203   91  283  1.00   19.63  19.63  0.00  18999 18999 1.00
  6    25  117  283  1.00   21.68  21.68  0.00  20989 20989 1.00
  7   258   90  304  1.00   20.45  20.45  0.00  19793 19793 1.00
  8    30  123  304  1.00   22.22  22.22  0.00  21513 21513 1.00
```

```
System working values:

  Image Xdim: 512 Ydim: 512, Pixsize: 1100

  Search Area xmin: 40 ymin: 200 xmax: 140 ymax: 320, Search Option: edge

  Ptile: Edge tile: 5, Ptile: 11, Offset: 20, Grid dim: 40, Thresh: 6,
  Range: 12, Mask1: 138, Mask2: 195
  Area1 SST: 21.38, Area2 SST: 20.25

  Stile: search dim: 40, offset: 1, Allowed RMS temp change: 6.00
  Allowed temp range from tile mean: 3.000, CC match(desired): 0.600,
  Flow rate(desired): 0.500, Max allowed flow: 0.800
```

Note the stile column in Search tile data. These are the number of reduced set search tiles (5 × 5) which met the selection criteria and were remapped and calculated for each pattern tile.

A.7 Image graphics

The graphics generated by this program covert pixels of the image to designated values. This makes the changes permanent as far as the output images are concerned. This is done to facilitate portability of the output images.

Additionally, a small pixel character map was written for this program to draw the date time group, tile labels and scales shown on the images.

Currently four images are output from this program:

- Pattern Tile Image (P-tiles written on the input image. Each tile is labeled with a text file identification number).

- Search Tile Image (Comparison image overwritten with p-tiles, selected s-tiles, and search box).

- Vector Image (Comparison image overwritten with magnitude and direction vectors . Each vector labeled with text file identification number).

- Arrow Image (Vector Image without the ID numbers).

Each output image is labeled with its date time group in the upper left corner, horizontal and vertical 0 - 30 kilometer scale in the lower right corner, and a vector magnitude arrow in meters per second.

Files which perform graphic operations are:

- graphics.c.

- label.c.

- line.c.

- veclabel.c.

A.8 Multiple image processing

When more than two images are available, they may be sequentially processed to track flow over time. After the initial two images are evaluated as previously described, a routine:

- swapfile.c.

is called which moves search tile data into pattern tile storage locations and calls the next specified image in as a search tile image. Search areas are recomputed based on the elapsed time between the new image pair, and the pattern search and vector computations are repeated. At the completion of each cycle, text and record images are generated.

Appendix B

PROGRAM CODE EXTRACTS

This appendix contains extracts from the current operating system which perform the tasks of selection, discrimination, and computation of surface flow.

B.1 Ordered statistical edge detection algorithm

The SEAD algorithm is executed in two parts: a reduced set search to locate an acceptable edge, and expanded mapping and verification for the desired pattern matching dimension.

B.1.1 Feature detection and discrimination

```
k=j+xdim*i;
count=0;
psum=0;
    for(N=0;N<(edgedim);++N)
        {
        for(M=0;M<(edgedim);++M)
          {
            l=k+N*xdim+M;
            shell0[count]=image[l];
            ptiles[ptilecount][count].i1 = i;
            ptiles[ptilecount][count].j1 = j;
            ptiles[ptilecount][count].k1 = k;
            ptiles[ptilecount][count].shell1 = shell0[count];
            psum=psum+shell0[count];
            count+=1;
          }
        }
        ptiles[ptilecount][0].psum1 = psum;
                /* stores total cell value for match in stile.c */

        ptiles[ptilecount][0].avgval1 = (int)((float)psum/(W));

                        /** rank pts **/
```

54

```
for(q=0;q<(W-2);++q)
    for(r=q+1;r<W-1;++r)
      {
        if(shell0[q]>shell0[r])
          {
            temp=shell0[q];
            shell0[q]=shell0[r];
            shell0[r]=temp;
          }
      }

    Range=shell0[W-1]-shell0[0];

                    /** Features are selected here for comparison.

                    Thresh is the threshold range for selection
                     as an edge.  A value of 5 says, that when
                     the subtiles are ordered by value, there must
                     be at least a value of 5 from highest to lowest

                    rng is the maximum separation allowed between
                     min and max subtile values. A low value but
                     must be greater than Thresh, discourages
                     selection of edges of great contrast such as
                     water and clouds.

                    mask1,mask2 are values for areas where edges
                     are not to be selected.  In this routine,
                     the value of the lowest ordered point
                     must be higher than the min mask value and
  the max value must be lower than the max mask
                    **/

if(Range>Thresh && Range<rng && shell0[0]> mask1
      && shell0[W]<mask2)

                    /* edge detected */
```

B.1.2   Pattern tile mapping and verification

```
K=k-tilediff-tilediff*xdim;
count=0;
psum=0;
  for(N=0;N<(tiledim);++N)
     {
     for(M=0;M<(tiledim);++M)
       {
       l=K+N*xdim+M;

       shell0[count]=image[l];
       ptiles[ptilecount][count].i = i;
       ptiles[ptilecount][count].j = j;
       ptiles[ptilecount][count].k = k;
       ptiles[ptilecount][count].shell = shell0[count];
       psum=psum+shell0[count];
       count+=1;
       }
     }
     ptiles[ptilecount][0].psum = psum;
               /* stores total cell value for match in stile.c */
     ptiles[ptilecount][0].avgval = (int)((float)psum/(WW));


/** Verify that all points in mapped
    feature lie within temperature
    range **/

     for(q=0;q<(WW);++q)
        for(r=q+1;r<WW;++r)
          {
          if(shell0[q]>shell0[r])
            {
            temp=shell0[q];
            shell0[q]=shell0[r];
            shell0[r]=temp;
            }
          }

     if(shell0[0]> mask1 && shell0[WW]<mask2)
            {
            ptilecount+=1;
            sw=1;
/** Apply offset to separate points **/
            if (j<jvalue)
              {
              j=j+offset;
              }
```

```
      else if (j>=jvalue)
       {
        j=jmax;
       }
     }
```

B.2 Subsequent feature recognition

Feature recognition is performed by performing a statistical correlation between reduced set tiles, and then full set comparisons. The reduced sets are compared just for correlation and mean temperature change. If they meet this criteria, the full pattern tile dimensions are then mapped and compared for correlation and points are ranked to insure that no points exceed the allowable temperature range.

B.2.1 Reduced set correlation

```
k=j+i*xdim;
count=0;
ssum=0;

for(N=0;N<(edgedim);++N)  /* searching each stile */
 {
   for(M=0;M<(edgedim);++M)
     {
       l=k+N*xdim+M;
       shelli[count]=image2[l];
       stiles[a+1][count].shelli = shelli[count];
       stiles[a+1][count].i = i;
       stiles[a+1][count].j = j;
       stiles[a+1][count].k = k;

       ssum=ssum+shelli[count];
       count+=1;
   }
 }

    /* defining values for mean avg sum match
     matchdel=((W)*sum(ptile*stile - sum[ptile]*sum[stile]) /
             sqrt((W)(sum[ptile]^2-(sum[ptile])^2))*
             ((W)(sum[stile]^2-(sum[stile])^2))         */
   sumy=ssum;
   sumx=ptiles[a][0].psum1;
   nsumxy=0;
   sumxsq=0;
   nsumxsq=0;
```

```
        sumsqx=0;
        sumysq=0;
        nsumysq=0;
        sumsqy=0;
        sumxy=0;

        for(c=0;c<W;++c)
        {
        sumxy=sumxy+(stiles[a+1][c].shell1*ptiles[a][c].shell1);
        }
        nsumxy=sumxy*(W);

        for(c=0;c<W;++c)
        {
        sumxsq=sumxsq+(ptiles[a][c].shell1*ptiles[a][c].shell1);
        sumysq=sumysq+
              (stiles[a+1][c].shell1*stiles[a+1][c].shell1);
        }
        nsumxsq=sumxsq*(W);
        nsumysq=sumysq*(W);

         sumsqx=sumx*sumx;
         sumsqy=sumy*sumy;

        numerator=nsumxy-(sumx*sumy);
        denominator=(float)sqrt((double)(nsumxsq-sumsqx)*(nsumysq-sumsqy));

        if (denominator == 0);
        {
         pdelsum=0;
        }

                                /** pdelsum is the correlation coeff.
                                    pccmatch is the desired minimum
                                     correlation
                                    tileratio is the rms error or
                                     difference between tiles
                                    temprng is the maximum deviation
                                     between tiles or across feature**/
        if(denominator != 0);
        {
        pdelsum=numerator/denominator;
        }
   if (pdelsum>=pccmatch && tileratio <= temprng)

             /*** Tile center meets corr. coeff, map full tile ***/
```

If the reduced set sample meets the conditional statement on the last line, the sample is remapped in a similar fashion to the pattern tile routine.

B.2.2 Search tile - pattern tile matching

The correlation for the expanded set is computed and the points are ranked using a routines similar to the ones above. The following criteria are applied for selection:

```
if ( pdelsum>=pccmatch && tileratio<=temprng
      && shell1[0]> srms-temprng/2 && shell1[WW]<srms+temprng/2)
```

This constrains selection to a specified correlation, maximum change in temperature due to diurnal heating, and a maximum temperature range for the tile.

B.3 Vector computations

Computation of vector magnitude and direction is a three step process. The values for the search tile x and y locations are subtracted from the pattern tile values and length (magnitude) is computed. Based on the values for the x and y sums, the routine selects a specific switch subroutine using the sign of the sums and the greater of their absolute values.

Vector length is determined by a simple Pythagorean routine:

```
vcomp = i-i2;                   /* x and y movement */
hcomp = j-j2;
length = (float)sqrt((double)(vcomp*vcomp + hcomp*hcomp));
```

Vector direction (anglea) is computed by determining the angle described by arccos $\frac{x}{r}$. The arrow head lines issue from the vector end at $45°$ angles from the line (angleb, anglec).

```
anglea = (float)acos((double)(h / length));
angleb=(pi/4)+anglea;
anglec=(pi/4)-anglea;
```

Direction is converted to degrees, flow rate is calculated, azimuth and arrow head endpoints are computed based on the region in which the vector is located (Figure A.2), and the image graphic is initiated with a function call as shown below:

```
                    /* conversion for radians to degrees */
#define degconv 57.29577951

vector[a].anglea=anglea*degconv;
vector[a].flow=(length*pixsize)/dtg[0].sec;
vector[a].anglea + ((float)(region value));


                            /** drawing vector **/
  i = ptiles[a][tilecenter].i;
  i1= select[a].i;
  j = ptiles[a][tilecenter].j;
  j1= select[a].j;

  draw_line(image,xdim,ydim,j,i,j1,i1,backvalue);


                        /** drawing arrow heads **/
        j2=j+icos;
        i2=i+isin;
        draw_line(image,xdim,ydim,j,i,j2,i2,backvalue);
        j2=j+icos1;
        i2=i-isin1;
        draw_line(image,xdim,ydim,j,i,j2,i2,backvalue);
```

Appendix C

THERMAL SIGNAL MAPS

This appendix contains image signal three dimensional representations generated using MATLAB for the mouth of the Delaware Bay. These figures are included to show the signal variations that are used by the SEDA algorithm to select features.

Cape May, New Jersey
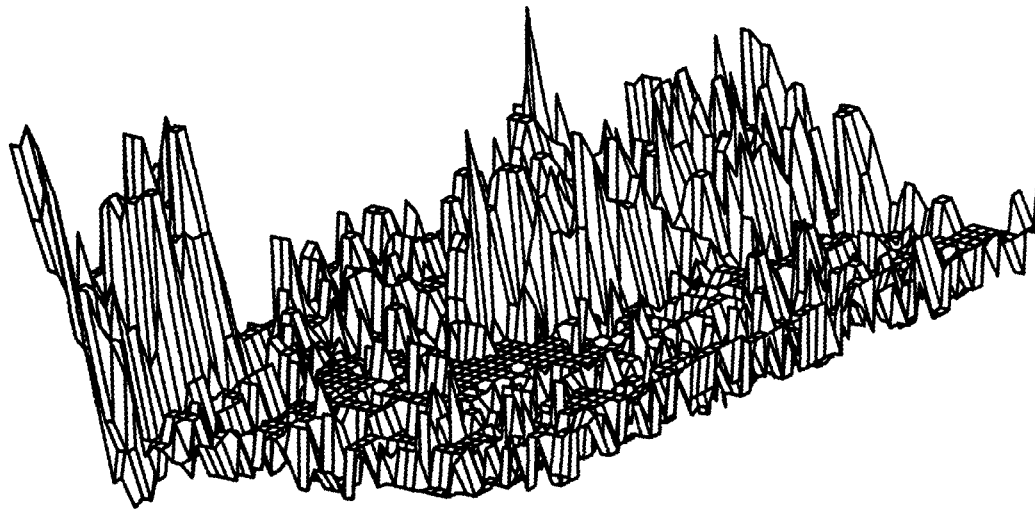
Thermal map: arbitrary scale, Azimuth: 315

Figure C.1: Thermal signal map, Delaware Bay and coastal region, 1100 hours local, 10 March 1989. Water signal spikes caused by vertical mixing of surface and subsurface waters.

Cape May, New Jersey
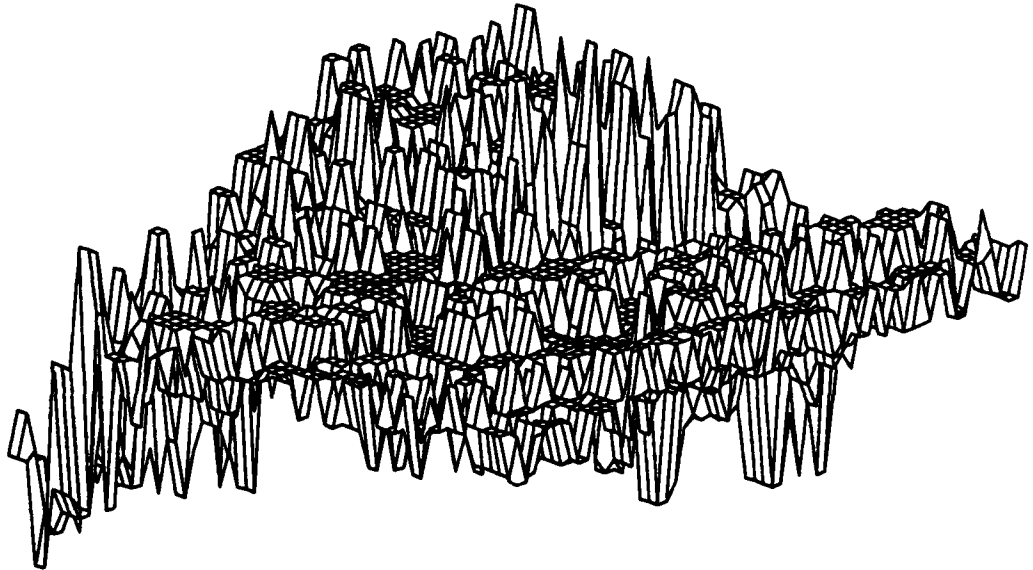
Thermal map: arbitrary scale, Azimuth: 315

Figure C.2: Thermal signal map, Delaware Bay and coastal region, 0100 hours local, 11 march 1989. Land and water signals are nearly indistinguishable due to low feature temperatures (5° C), which are approaching the lower signal threshold for the image.

Cape May, New Jersey
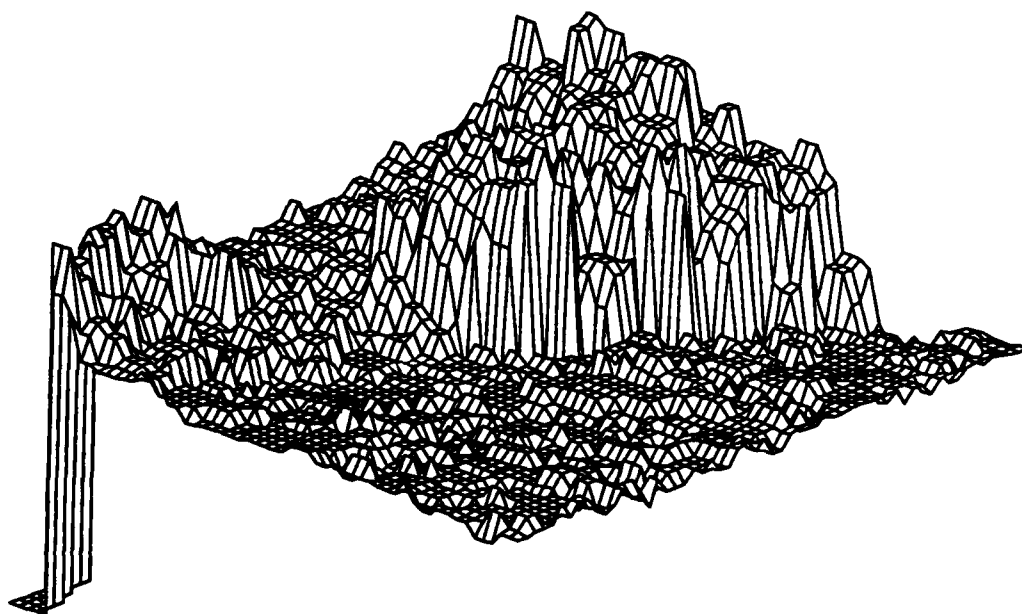
Thermal map: arbitrary scale, Azimuth: 315

Figure C.3: Thermal signal map, Delaware Bay and coastal region, 1158 hours local, 28 May 1989. Smooth ocean signal surface indicates formation of a surface mixed layer. Elevated land signals are due to higher incident solar flux and seasonal warming. Extremely low values on left edge were caused by clouds over Lewes, Delaware.

Cape May, New Jersey
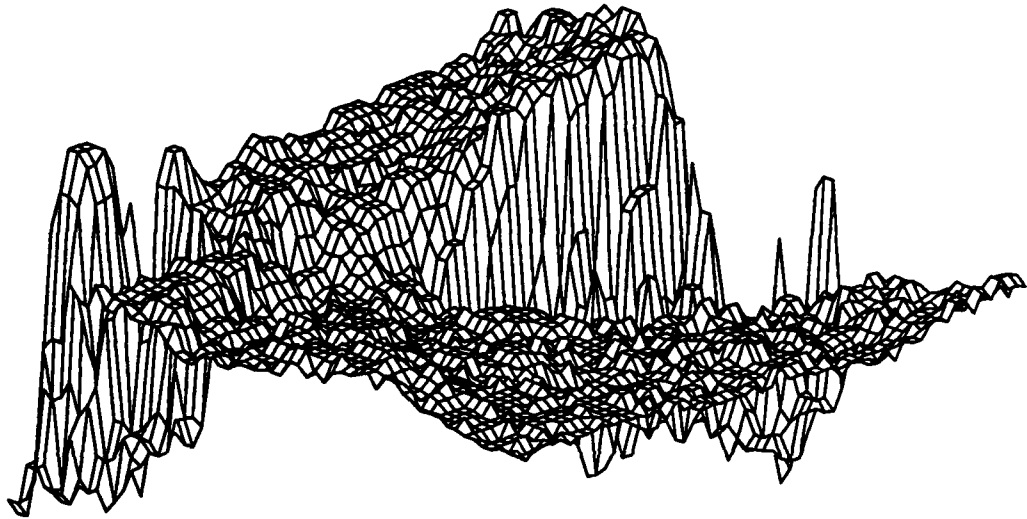
Thermal map: arbitrary scale, Azimuth: 315

Figure C.4: Thermal signal map, Delaware Bay and coastal region, 0201 hours local, 29 May 1989. Land temperatures lower due to diurnal heat loss.

Cape May, New Jersey
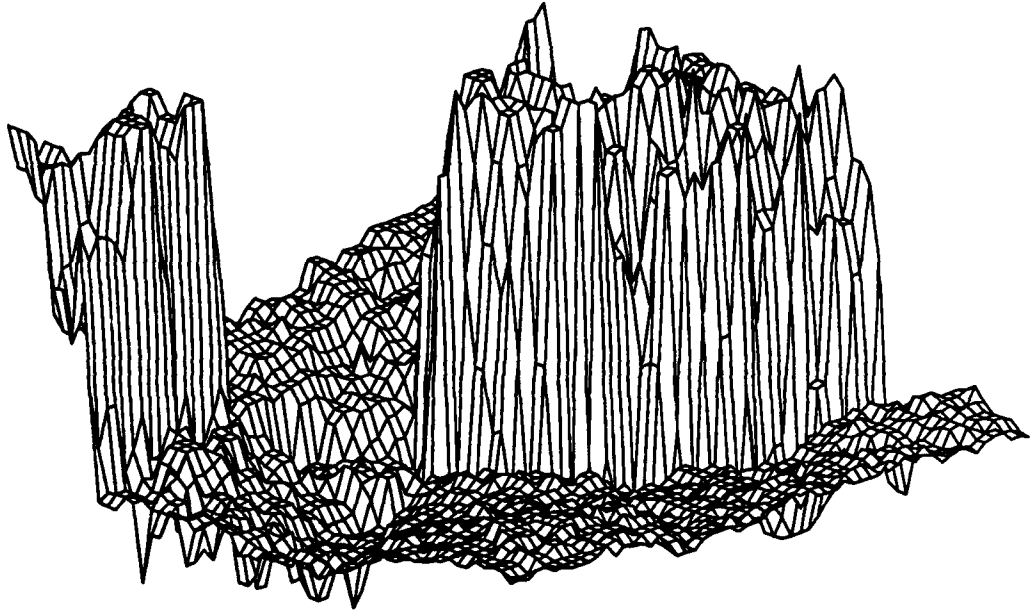
Thermal map: arbitrary scale, Azimuth: 315

Figure C.5: Thermal signal map, Delaware Bay and coastal region, 1303 hours local, 10 June 1989. High land and low water signals due to diurnal heating from increased incident solar flux.

Cape May, New Jersey
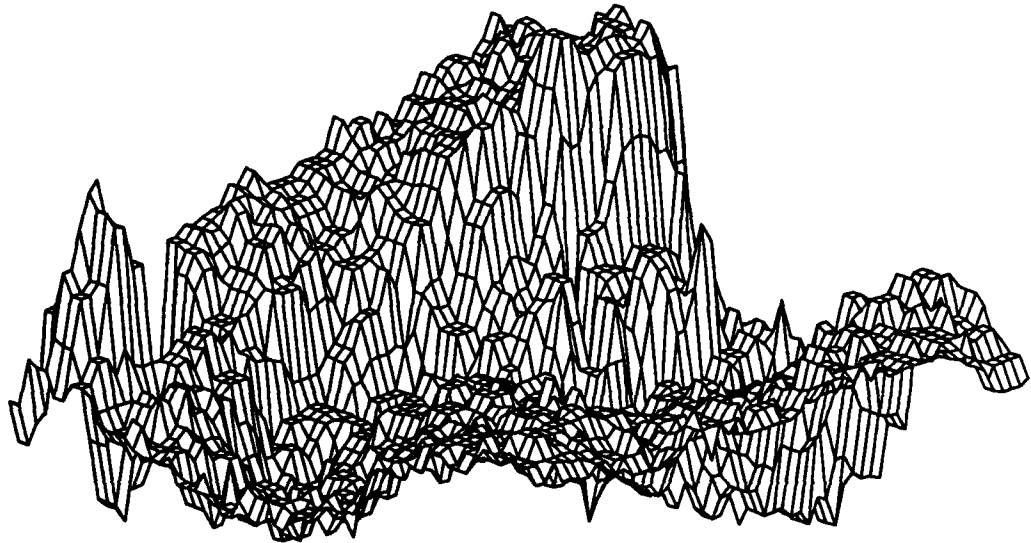
Thermal map: arbitrary scale, Azimuth: 315

Figure C.6: Thermal signal map, Delaware Bay and coastal region, 0117 hours local, 11 June 1989. Land values are lower water due to diurnal heat loss. Delaware Bay temperatures (rear) are 2-3° C higher than coastal waters (foreground).

Cape May, New Jersey
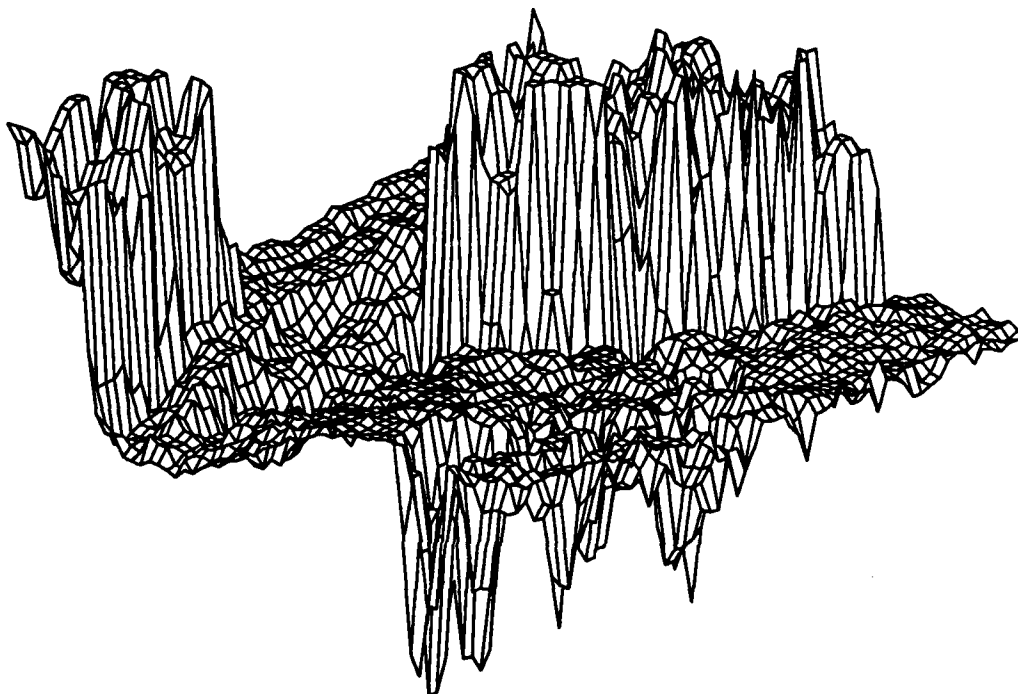
Thermal map: arbitrary scale, Azimuth: 315

Figure C.7: Thermal signal map, Delaware Bay and coastal region, 1308 hours local, 29 June 1989. Signal drop in foreground due to clouds.

Appendix D

TABULAR DATA

This appendix contains tabular output data for one program run in the period specified in the Delaware Bay area. Each data set is comprised of three parts:

- Vector direction and magnitude information

- Search tile - pattern tile correlation information

- Program run parameters

D.1   10-11 March 1989

From: 89069170021, To: 89069184155:
Elapsed time: 0 Day(s), Total: 1 Hours, 41 Minutes, 34 Seconds
Search box dim:15 Offset: 10 Tile dim: 11 X 11 Number of samples 31

pt	lngth(km)	az(deg)	flow m/s
0	0.00	0.00	0.00
1	0.00	0.00	0.00
2	0.00	0.00	0.00
3	0.00	0.00	0.00
4	0.00	0.00	0.00
5	0.00	0.00	0.00
6	0.00	0.00	0.00
7	0.00	0.00	0.00
8	0.00	0.00	0.00
9	0.00	0.00	0.00
10	0.00	0.00	0.00
11	0.00	0.00	0.00
12	0.00	0.00	0.00
13	0.00	0.00	0.00
14	0.00	0.00	0.00
15	0.00	0.00	0.00
16	0.00	0.00	0.00
17	0.00	0.00	0.00
18	0.00	0.00	0.00
19	0.00	0.00	0.00

```
20   0.00       0.00     0.00
21   0.00       0.00     0.00
22   0.00       0.00     0.00
23   0.00       0.00     0.00
24   0.00       0.00     0.00
25   0.00       0.00     0.00
26   0.00       0.00     0.00
27   0.00       0.00     0.00
28   0.00       0.00     0.00
29   0.00       0.00     0.00
30   0.00       0.00     0.00
```

Average flow distance: 0.00 km, Avg Az: 0.00 deg, Avg flow rate: 0.00 m/s

Search tile data (x,y coord for center subtile)

ptile	stile	x	y	CC val	Pt temp	St temp	del T	Pt sum	St sum	Ratio
0	0	137	221	0.45	5.05	4.26	0.79	4892	4125	1.19
1	0	0	0	0.00	0.00	0.00	0.00	4793	0	0.00
2	0	0	0	0.00	0.00	0.00	0.00	5249	0	0.00
3	0	0	0	0.00	0.00	0.00	0.00	5318	0	0.00
4	0	0	0	0.00	0.00	0.00	0.00	4818	0	0.00
5	0	119	243	0.10	4.97	3.54	1.44	4815	3424	1.41
6	0	130	243	0.12	5.38	4.56	0.82	5210	4414	1.18
7	0	70	254	0.50	5.50	2.82	2.68	5327	2732	1.95
8	0	109	254	0.30	4.80	3.48	1.32	4643	3367	1.38
9	0	120	254	0.00	4.89	4.29	0.60	4730	4152	1.14
10	0	79	265	0.32	4.57	3.04	1.53	4421	2938	1.50
11	0	0	0	0.00	0.00	0.00	0.00	4504	0	0.00
12	0	122	265	0.25	4.87	4.46	0.42	4718	4315	1.09
13	0	0	0	0.00	0.00	0.00	0.00	5523	0	0.00
14	0	87	276	0.20	4.63	3.47	1.16	4482	3360	1.33
15	0	0	0	0.00	0.00	0.00	0.00	4282	0	0.00
16	0	115	276	0.15	4.72	4.06	0.66	4572	3930	1.16
17	0	0	0	0.00	0.00	0.00	0.00	5085	0	0.00
18	0	0	0	0.00	0.00	0.00	0.00	5525	0	0.00
19	0	0	0	0.00	0.00	0.00	0.00	4349	0	0.00
20	0	108	287	0.03	4.50	3.56	0.94	4356	3450	1.26
21	0	120	287	0.02	4.56	4.01	0.55	4418	3881	1.14
22	0	0	0	0.00	0.00	0.00	0.00	5379	0	0.00
23	0	0	0	0.00	0.00	0.00	0.00	4176	0	0.00
24	0	0	0	0.00	0.00	0.00	0.00	4273	0	0.00
25	0	0	0	0.00	0.00	0.00	0.00	4875	0	0.00
26	0	0	0	0.00	0.00	0.00	0.00	5402	0	0.00
27	0	91	309	0.12	4.31	3.56	0.74	4168	3447	1.21
28	0	104	309	0.25	4.44	3.76	0.69	4301	3635	1.18
29	0	115	309	0.41	4.91	3.31	1.59	4751	3208	1.48
30	0	0	0	0.00	0.00	0.00	0.00	5671	0	0.00

System working values:

Image Xdim: 512 Ydim: 512, Pixsize: 1100

Search Area xmin: 40 ymin: 200 xmax: 140 ymax: 320, Search Option: edge

Ptile: Edge tile: 5, Ptile: 11, Offset: 10, Grid dim: 40, Thresh: 6,
Range: 12, Mask1: 26, Mask2: 61
Area1 SST: 5.62, Area2 SST: 5.25

Stile: search dim: 4, offset: 1, Allowed RMS temp change: 4.00
Allowed temp range from tile mean: 2.000, CC match(desired): 0.600,
Flow rate(desired): 0.500, Max allowed flow: 0.800

D.2 28-29 May 1989

From: 89148165803, To: 89149070111:
Elapsed time: 1 Day(s), Total: 9 Hours, 57 Minutes, 8 Seconds
Search box dim:103 Offset: 10 Tile dim: 11 X 11 Number of samples 22

pt	lngth(km)	az(deg)	flow m/s
0	48.27	39.96	0.92
1	59.46	137.73	1.14
2	51.74	131.08	0.99
3	0.00	0.00	0.00
4	0.00	0.00	0.00
5	23.00	180.00	0.44
6	0.00	0.00	0.00
7	49.04	129.21	0.94
8	57.49	130.06	1.10
9	0.00	0.00	0.00
10	0.00	0.00	0.00
11	41.19	5.57	0.79
12	52.80	142.70	1.01
13	0.00	0.00	0.00
14	0.00	0.00	0.00
15	0.00	0.00	0.00
16	0.00	0.00	0.00
17	15.62	129.81	0.30
18	0.00	0.00	0.00
19	0.00	0.00	0.00
20	47.80	164.22	0.92
21	0.00	0.00	0.00

Average flow distance: 13.73 km, Avg Az: 126.76 deg, Avg flow rate: 0.26 m/s

Search tile data (x,y coord for center subtile)

ptile	stile	x	y	CC val	Pt temp	St temp	del T	Pt sum	St sum	Ratio
0	81	153	195	0.88	12.01	12.30	-0.30	11621	11909	0.98
1	116	103	287	0.72	16.44	14.58	1.86	15915	14110	1.13
2	33	105	288	0.63	15.34	14.69	0.65	14847	14222	1.04
3	0	119	254	0.02	12.86	13.71	-0.85	12447	13268	0.94
4	0	65	265	0.51	14.96	11.21	3.75	14485	10856	1.33
5	14	106	288	0.64	12.31	14.70	-2.39	11915	14231	0.84
6	1	125	265	0.28	12.89	13.17	-0.27	12481	12747	0.98
7	44	113	307	0.63	13.40	14.93	-1.53	12972	14450	0.90
8	609	150	313	0.70	11.74	13.59	-1.86	11363	13159	0.86
9	0	119	276	0.17	12.30	12.40	-0.09	11908	11999	0.99
10	0	135	276	0.24	12.96	13.42	-0.46	12550	12995	0.97
11	19	79	246	0.78	14.19	17.20	-3.01	13740	16651	0.83
12	62	122	329	0.64	12.33	13.96	-1.62	11938	13511	0.88
13	0	101	287	0.04	12.45	16.08	-3.63	12055	15566	0.77
14	0	117	287	0.15	12.43	12.50	-0.07	12028	12099	0.99
15	0	107	298	0.23	13.03	14.29	-1.26	12614	13829	0.91
16	0	125	298	0.17	12.20	13.18	-0.98	11813	12762	0.93
17	63	148	308	0.60	12.30	14.01	-1.72	11902	13563	0.88

```
18     0   86  309  0.28     13.89    11.69  2.20  13444  11316 1.19
19     0   98  309  0.04     13.42     9.98  3.44  12992   9663 1.34
20   715  122  355  0.79     13.16    14.35 -1.19  12741  13889 0.92
21     0  128  309  0.05     11.87    11.74  0.13  11490  11366 1.01
```

System working values:

Image Xdim: 512 Ydim: 512, Pixsize: 1100

Search Area xmin: 40 ymin: 200 xmax: 140 ymax: 320, Search Option: edge

Ptile: Edge tile: 5, Ptile: 11, Offset: 10, Grid dim: 40, Thresh: 6,
Range: 12, Mask1: 85, Mask2: 140
Area1 SST: 15.50, Area2 SST: 12.63

Stile: search dim: 92, offset: 1, Allowed RMS temp change: 4.00
Allowed temp range from tile mean: 2.000, CC match(desired): 0.600,
Flow rate(desired): 0.900, Max allowed flow: 1.500

D.3 10-12 June 1989

Elapsed time: 1 Day(s), Total: 12 Hours, 25 Minutes, 19 Seconds
Search box dim:83 Offset: 10 Tile dim: 11 X 11 Number of samples 19

pt	lngth(km)	az(deg)	flow m/s
0	0.00	0.00	0.00
1	0.00	0.00	0.00
2	4.00	180.00	0.10
3	11.05	95.19	0.27
4	0.00	0.00	0.00
5	3.00	180.00	0.07
6	7.00	180.00	0.17
7	21.26	48.81	0.52
8	0.00	0.00	0.00
9	7.07	171.87	0.17
10	39.85	197.53	0.98
11	0.00	0.00	0.00
12	37.34	172.30	0.92
13	9.22	319.40	0.23
14	27.46	169.51	0.68
15	12.00	180.00	0.30
16	31.30	26.57	0.77
17	5.39	201.80	0.13
18	36.25	24.44	0.89

Average flow distance: 3.77 km, Avg Az: 141.46 deg, Avg flow rate: 0.09 m/s

Search tile data (x,y coord for center subtile)

ptile	stile	x	y	CC val	Pt temp	St temp	del T	Pt sum	St sum	Ratio
0	0	0	0	0.00	0.00	0.00	0.00	25302	0	0.00
1	0	0	0	0.00	0.00	0.00	0.00	26832	0	0.00
2	163	123	236	0.62	18.70	16.11	2.58	18099	15599	1.16
3	98	147	233	0.81	18.50	16.34	2.16	17912	15820	1.13
4	0	0	0	0.00	0.00	0.00	0.00	21696	0	0.00
5	135	74	246	0.65	22.12	19.75	2.38	21414	19115	1.12
6	192	116	250	0.64	18.46	16.44	2.02	17866	15911	1.12
7	8	149	229	0.75	19.03	16.09	2.94	18423	15575	1.18
8	0	0	0	0.00	0.00	0.00	0.00	23563	0	0.00
9	45	66	261	0.66	21.05	18.35	2.69	20372	17767	1.15
10	559	102	292	0.87	17.80	15.19	2.61	17231	14701	1.17
11	0	0	0	0.00	0.00	0.00	0.00	23675	0	0.00
12	138	114	302	0.69	17.57	17.50	0.07	17006	16938	1.00
13	116	114	258	0.83	18.57	15.89	2.67	17971	15383	1.17
14	191	111	303	0.74	17.96	17.20	0.75	17381	16654	1.04
15	199	106	299	0.90	18.38	16.12	2.26	17796	15607	1.14
16	78	107	270	0.66	17.55	15.63	1.92	16990	15133	1.12
17	161	103	303	0.88	18.57	15.73	2.84	17973	15225	1.18
18	16	107	276	0.69	17.92	16.24	1.68	17351	15723	1.10

System working values:

Image Xdim: 512 Ydim: 512, Pixsize: 1100

Search Area xmin: 40 ymin: 200 xmax: 140 ymax: 320, Search Option: edge

Ptile: Edge tile: 5, Ptile: 11, Offset: 10, Grid dim: 40, Thresh: 6,
Range: 12, Mask1: 132, Mask2: 182
Area1 SST: 21.25, Area2 SST: 18.00

Stile: search dim: 72, offset: 1, Allowed RMS temp change: 3.00
Allowed temp range from tile mean: 1.500, CC match(desired): 0.600,
Flow rate(desired): 0.900, Max allowed flow: 1.500

D.4   29-30 June 1989

From: 89180180847,   To: 89181063256:
Elapsed time: 1 Day(s), Total: 12 Hours, 24 Minutes, 9 Seconds
Search box dim:83 Offset: 10 Tile dim: 11 X 11 Number of samples 26

pt	lngth(km)	az(deg)	flow m/s
0	0.00	0.00	0.00
1	0.00	0.00	0.00
2	0.00	0.00	0.00
3	23.71	152.35	0.58
4	23.41	160.02	0.58
5	43.14	45.94	1.06
6	0.00	0.00	0.00
7	41.11	48.95	1.01
8	0.00	0.00	0.00
9	1.00	180.00	0.02
10	0.00	0.00	0.00
11	45.80	53.88	1.13
12	0.00	0.00	0.00
13	24.76	46.64	0.61
14	2.24	153.43	0.06
15	0.00	0.00	0.00
16	0.00	0.00	0.00
17	50.45	50.63	1.24
18	19.31	158.75	0.48
19	0.00	0.00	0.00
20	4.00	360.00	0.10
21	5.00	216.87	0.12
22	21.00	360.00	0.52
23	23.77	337.75	0.59
24	10.00	143.13	0.25
25	26.02	357.80	0.64

Average flow distance: 8.10 km, Avg Az: 53.55 deg, Avg flow rate: 0.20 m/s

Search tile data (x,y coord for center subtile)

ptile	stile	x	y	CC val	Pt temp	St temp	del T	Pt sum	St sum	Ratio
0	14	66	210	0.24	27.40	22.67	4.73	26528	21949	1.21
1	99	81	210	0.27	28.61	24.08	4.53	27695	23312	1.19
2	109	119	210	0.05	26.12	21.22	4.90	25284	20544	1.23
3	391	72	253	0.82	24.42	21.54	2.88	23642	20851	1.13
4	583	76	265	0.82	22.87	20.02	2.85	22136	19376	1.14
5	35	137	213	0.63	22.02	18.90	3.12	21319	18295	1.17
6	0	118	243	0.06	21.36	18.83	2.54	20679	18224	1.13
7	53	168	216	0.68	20.81	21.00	-0.19	20143	20327	0.99
8	0	50	254	0.41	25.61	22.54	3.06	24789	21823	1.14
9	484	73	255	0.90	21.83	21.43	0.40	21133	20742	1.02
10	22	92	254	0.17	27.02	22.22	4.80	26151	21509	1.22
11	79	145	227	0.64	20.51	20.29	0.22	19855	19641	1.01
12	1	120	254	0.11	21.14	18.53	2.61	20468	17938	1.14
13	101	76	248	0.85	24.59	22.86	1.74	23806	22124	1.08

14	425	76	267	0.89	20.40	19.60	0.80	19752	18975	1.04
15	2	91	265	0.19	20.34	16.33	4.01	19687	15808	1.25
16	0	104	265	0.05	20.17	19.97	0.20	19529	19332	1.01
17	3	163	233	0.67	21.04	21.90	-0.85	20371	21197	0.96
18	396	88	294	0.84	18.27	19.23	-0.96	17681	18614	0.95
19	0	70	287	0.05	26.82	22.80	4.03	25965	22067	1.18
20	4	82	283	0.80	18.20	18.15	0.06	17621	17566	1.00
21	129	91	291	0.92	20.24	19.90	0.34	19592	19262	1.02
22	150	82	277	0.70	18.13	18.11	0.01	17545	17534	1.00
23	100	129	276	0.61	21.83	21.53	0.31	21136	20837	1.01
24	13	87	317	0.63	18.53	19.48	-0.96	17934	18859	0.95
25	4	91	283	0.84	20.56	19.63	0.93	19904	18999	1.05

System working values:

Image Xdim: 512 Ydim: 512, Pixsize: 1100

Search Area xmin: 40 ymin: 200 xmax: 140 ymax: 320, Search Option: edge

Ptile: Edge tile: 5, Ptile: 11, Offset: 10, Grid dim: 40, Thresh: 6,
Range: 12, Mask1: 124, Mask2: 196
Area1 SST: 22.00, Area2 SST: 18.00

Stile: search dim: 72, offset: 1, Allowed RMS temp change: 5.00
Allowed temp range from tile mean: 2.500, CC match(desired): 0.600,
Flow rate(desired): 0.900, Max allowed flow: 1.500

REFERENCES

[1] Vastano, A. C., and R. O. Reid. "Sea Surface Topography Estimation with Infrared Satellite Imagery." *Journal of Atmospheric and Oceanic Technology*, 2:393-400, September 1985.

[2] Stewart, R. H.. "Methods of Satellite Oceanography." University of California Press, Los Angeles, 1985.

[3] Wahl, D. D., and J. J. Simpson. "Physical Processes Affecting the Objective Determination of Near - Surface Velocity From Satellite Data." *Journal of Geophysical Research*, 95(C8):13,511-13,528, August 1990.

[4] Price, J. F., R. A. Weller and R. Pinkel. "Diurnal Cycling: Observations and Models of the Upper Ocean Response to Diurnal Heating, Cooling and Wind Mixing." *Journal of Geophysical Research*, 91(C7):8411-8427, July 1986.

[5] Kelly, K. A.. "An Inverse Model for Near Surface Velocity from Infrared Images." *Journal of Physical Oceanography*, 19(12):1845-1864, December 1989.

[6] Simpson, J. J., and J. Bloom. "Objective Determination of Near - Surface Velocity form Spacecraft using Minimum Distortion and Log Search Methods." Scripts Institution of Oceanography, May 1990.

[7] Hardie, R. C., and R. Gnacek. "Robust Ranked - Order Based Vector Edge Detectors for Color Image Processing." Department of Electrical Engineering, University of Delaware, Newark DE, April 1990.

[8] Pitas, I., A. N. Venetsanopoulos. "Edge Detectors Based on Order Statistics." *IEEE Transactions on Pattern Analysis and Machine Intelligence*, PAMI-8(4):538-550, July 1986.

[9] Fukunaga, K.. "Introduction to Statistical Pattern Recognition, Second Edition." Academic Press, San Diego, 1990.

[10] Lim, J. S.. "Two - Dimensional Signal and Image Processing." Prentice Hall, Englewood Cliffs, 1990.

[11] Rosenfeld, A., Editor. "Digital Picture Analysis." Springer - Verlag, New York, 1976.

[12] Emery, W. J., A. C. Thomas, M. J. Collins, W. R. Crawford and D. L. Mackas. "An Objective Method for Computing Advective Surface Velocities form Sequential Infrared Satellite Images." *Journal of Geophysical Research*, 91:12,865-12,878, November 1986.

[13] Baker, L.. "More C Tools for Scientists and Engineers." McGraw Hill, New York, 1991.

[14] Simpson, J. J., and C. Humphrey. "An Automated Cloud Screening Algorithm or Daytime Advanced Very High Resolution Radiometer Imagery." *Journal of Geophysical Research*, 95(C8):13,459-13,481, August 1990.

[15] Gautier, C., G. Diak, S. Masse. "A Simple Physical Model to Estimate Incident Solar Radiation at the Surface from GOES Satellite Data." *Journal of Applied Meteorology*, 19:1005-1012, August 1990.

[16] Münchow, A., A. K. Masse and R. W. Garvine. "Astronomical and Nonlinear Tidal Currents in a Coupled Estuary Shelf System." Paper submitted to: *Continental Shelf Research*, December 1990.

[17] Yan, X. H., J. R. Schubel and D. W. Pritchard. "Oceanic Upper Mixed Layer Depth Determination by the Use of Satellite Data." *Remote Sensing of the Environment*, 32(1):55-74, April 1990.

[18] Yan, X. H., A. Okubo, J. R. Schubel and D. W. Pritchard. "An Analytical model for Remote Sensing Determination of the Mixed Layer Depth." Paper submitted to: *Deep - Sea Research*, June 1990.

[19] "IVAS Display Processor." International Imaging Systems, Milpitas, CA.

[20] Little, J. N. and L. Shure. "PRO - MATLAB Users Guide." The Math Works, Inc., South Natick, MA, January 1989.

[21] Canny, J.. "A Computational Approach to Edge Detection." *IEEE Transactions on Pattern analysis and Machine Intelligence*, PAMI-8(6):679-698, November 1986.

[22] Dougherty, E., and C. Giardina. "Matrix Structured Image Processing." Prentice Hall, Englewood Cliffs, 1987.

[23] Münchow, A., R. W. Garvine and T. F. Pfeiffer. "Subtidal Currents from a Shipboard Acoustic Doppler Current Profiler in Tidally Dominated Waters." Paper submitted to: *Continental Shelf Research*, January 1991.

[24] Selby, S.. "CRC Handbook of Standard Mathematical Tables." 19th Edition, CRC Press, Cleveland, 1971.

[25] Simpson, J. J., and R. J. Lynn. "A Mesoscal Eddy Dipole in the Offshore California Current." *Journal of Geophysical Research*, 95(C8):13,009-13,022, August 1990.

[26] Vastano, A. C., S. E. Borders and R. E. Wittenberg. "Sea Surface Flow Estimation with Infrared and Visible Imagery." *Journal of Atmospheric and Oceanic Technology*, 2:401-403, September 1985.

[27] Wahl, D. D., and J. J. Simpson. "Satellite Derived Estimates of the Normal and Tangential Components of Near Surface Flow." Paper submitted to the International Journal of Remote Sensing, 1990.